Effects of External Rb^+ on Inward Rectifier K^+ Channels of Bovine Pulmonary Artery Endothelial Cells

MICHAEL R. SILVER*, MARK S. SHAPIRO, and THOMAS E. DECOURSEY

From the Departments of *Medicine and Physiology, Rush-Presbyterian-St. Luke's Medical Center, Chicago, Illinois 60612

ABSTRACT Inward rectifier (IR) K^+ channels of bovine pulmonary artery endothelial cells were studied using the whole-cell, cell-attached, and outside-out patch-clamp configurations. The effects of Rb^+ on the voltage dependence and kinetics of IR gating were explored, with $[Rb^+]_o + [K^+]_o = 160$ mM. Partial substitution of Rb^+ for K^+ resulted in voltage-dependent reduction of inward currents, consistent with Rb^+ being a weakly permeant blocker of the IR. In cells studied with a K^+-free pipette solution, external Rb^+ reduced inward IR currents to a similar extent at large negative potentials but block at more positive potentials was enhanced. In outside-out patches, the single-channel i-V relationship was approximately linear in symmetrical K^+, but rectified strongly outwardly in high $[Rb^+]_o$ due to a reduced conductance for inward current. The permeability of Rb^+ based on reversal potential, V_{rev}, was 0.45 that of K^+, whereas the Rb^+ conductance was much lower, 0.034 that of K^+, measured at V_{rev}-80 mV. The steady state voltage-dependence of IR gating was determined in Rb^+-containing solutions by applying variable prepulses, followed by a test pulse to a potential at which *outward* current deactivation was observed. As $[Rb^+]_o$ was increased, the half-activation potential, $V_{1/2}$, changed less than V_{rev}. In high $[K^+]_o$ solutions $V_{1/2}$ was V_{rev}-6 mV, while in high $[Rb^+]_o$ $V_{1/2}$ was V_{rev} + 7 mV. This behavior contrasts with the classical parallel shift of $V_{1/2}$ with V_{rev} in K^+ solutions. Steady state IR gating was less steeply voltage-dependent in high $[Rb^+]_o$ than in K^+ solutions, with Boltzmann slope factors of 6.4 and 4.4 mV, respectively. Rb^+ decreased (slowed) both activation and deactivation rate constants defined at $V_{1/2}$, and decreased the steepness of the voltage dependence of the activation rate constant by 42%. Deactivation of IR channels in outside-out patches was also slowed by Rb^+. In summary, Rb^+ can replace K^+ in setting the voltage-dependence of IR gating, but in doing so alters the kinetics.

Address correspondence to Dr. Thomas E. DeCoursey, Department of Physiology, Rush-Presbyterian-St. Luke's Medical Center, 1653 West Congress Parkway, Chicago, IL 60612.

Dr. Shapiro's present address is Department of Physiology and Biophysics, SJ-40, University of Washington, Seattle, WA 98195.

J. GEN. PHYSIOL. © The Rockefeller University Press · 0022-1295/94/04/0519/30 $2.00
Volume 103 April 1994 519–548

INTRODUCTION

The mechanism of gating of inward rectifier (IR) channels appears to differ qualitatively from that of other voltage-dependent ion channels. Whereas mostvoltage-gated ion channels are envisioned as opening and closing as a direct result of voltage-induced alterations in the structural configuration of the channel protein, the voltage-dependence of IR channel gating is profoundly affected by the concentration of permeant ions, and thus most likely arises from a distinct mechanism. Major structural differences between a recently cloned IR channel (Kubo, Baldwin, Jan, and Jan, 1993) and a large group of structurally similar voltage-gated K^+ channels are consistent with the possibility that these two classes of channels may have distinct gating mechanisms. The voltage-dependence of the IR was first described as a strict function of the extracellular K^+ concentration, $[K^+]_o$, such that rectification depended on the reversal potential for K^+, E_K (Hodgkin and Horowicz, 1959; Almers, 1971; Hagiwara and Takahashi, 1974). A distinction was made between instantaneous rectification of the IR and a voltage- and time-dependent gating mechanism (Almers, 1971; Hagiwara, Miyazaki, and Rosenthal, 1976; Leech and Stanfield, 1981; Hestrin, 1981; DeCoursey, Dempster, and Hutter, 1984). Changes in intracellular K^+ concentration, $[K^+]_i$, were shown to affect the position of the voltage-activation curve of the IR, although less profoundly than changes in $[K^+]_o$ (Hagiwara and Yoshii, 1979; Hestrin, 1981; Saigusa and Matsuda, 1988; Cohen, DiFrancesco, Mulrine, and Pennefather, 1989; Pennefather, Oliva, and Mulrine, 1992). It has thus been possible to dissociate shifts in the position of the voltage-activation curve from shifts in V_{rev}. Pennefather et al. (1992) proposed that inward rectification is not an intrinsic property of the single IR channel conductance, but rather that rectification results from a voltage-dependent isomerization that is intrinsic to the channel protein, and that is modulated by allosteric regulatory binding sites for K^+ on the outside of the channel.

In the past decade, permeant ion effects on gating have been demonstrated in a number of ion channels (references cited in Shapiro and DeCoursey, 1991*b*). The effects of permeant ions on the gating of other channels are more subtle than the effects of $[K^+]_o$ on the IR, and generally have been viewed as modulation of a gating mechanism which is intrinsic to the channel protein, rather than as evidence that gating itself might be due to interaction of permeant ions with the channel (Chen and Eisenberg, 1992). In addition to the profound effects of $[K^+]_o$ on IR gating, when Tl^+ replaces K^+ in the external solution, activation of IR currents becomes faster (Hagiwara, Miyazaki, Krasne, and Ciani, 1977) and an inactivation process occurs upon hyperpolarization (Stanfield, Ashcroft, and Plant, 1981). The permeant blockers of cardiac I_{K1} channels, Rb^+ and Cs^+, slow activation (Tourneur, Mitra, Morad, and Rougier, 1987; Mitra and Morad, 1991) and result in I_{K1} current "inactivation," which appears to represent block by external divalent cations, in cells dialyzed with K^+-free solution (Mitra and Morad, 1991).

We have studied the relationship between $[Rb^+]_o$ and the IR gating mechanism in bovine pulmonary artery endothelial cells. Under the ionic conditions employed, the IR is the predominant ionic conductance present, and this combined with their small size and favorable geometry (compared with myocytes, for example), makes endothe-

lial cells a nearly ideal preparation for these studies. Rb^+ blocks inward K^+ currents in a voltage-dependent manner, but is also weakly conductive. At the single channel level, Rb^+ reduces the apparent unitary current amplitude, presumably due to block with rapid kinetics. A major result of the present study is that Rb^+, like K^+, can "set" the position on the voltage axis of the voltage-activation curve of the IR channel. We demonstrate that as the Rb^+ mole-fraction is increased, the midpoint of the macroscopically observable gating process does not shift to the same extent as V_{rev}. As a result, in high $[Rb^+]_o$ most of the channels are open at V_{rev}, whereas in high $[K^+]_o$ most of the channels are closed at V_{rev}. In addition, Rb^+ slows the kinetics of gating. Thus, in high $[Rb^+]_o$ it is possible to observe large and relatively slowly decaying transient outward IR currents during depolarizing voltage pulses from potentials at which the IR conductance was activated. This phenomenon is exploited to quantify the voltage-dependence of the IR gating mechanism over the full range of Rb^+ and K^+ mole fractions. External Rb^+ slows IR gating. The steady state activation curve is less steep in high $[Rb^+]_o$, which in terms of a simple two-state model can be ascribed to a decrease in the steepness of the voltage-dependence of the activation rate. These effects of Rb^+ are interpreted with respect to a quantitative model of gating in a companion paper (Pennefather and DeCoursey, 1994).

MATERIALS AND METHODS

Cells

The techniques used for isolation, culture, and identification of bovine pulmonary artery endothelial cells were described previously (Silver and DeCoursey, 1990). Briefly, endothelial cells were isolated from bovine pulmonary arteries obtained from a slaughterhouse, by enzymatic digestion: 0.25% collagenase (Worthington CL-II, Cooper Biomedical, Malvern, PA) incubated for 30 min at 37°C. Cells were studied from passage 3 through 9. Cells were plated onto fragments of glass cover slips before electrophysiologic study, in order to facilitate transfer into the recording chamber.

Solutions

The composition of the solutions used are given in Table I*A* and *B*. Solutions are indicated in the text according to their monovalent cation constituents in mM: *e.g.*, 40 K + 120 Rb. The pipette solution used in most whole-cell experiments was KCH_3SO_3, and was nominally Mg^{2+}-free in order to minimize possible block of outward current (Vandenberg, 1987; Matsuda, Saigusa, and Irisawa, 1987) and interaction with the gating mechanism (Matsuda, 1988; Oliva, Cohen, and Pennefather, 1990; Silver and DeCoursey, 1990; Pennefather *et al.*, 1992). Liquid junction potentials arising between the pipette solution and the bath solution and between the reference electrode and the bath solution were calculated as described previously (Silver and DeCoursey, 1990; Shapiro and DeCoursey, 1991*a*), and were < 5.2 mV in all experiments. Data presented in tables and in Figs. 6–12 have been corrected, except Fig. 10, while other raw data are illustrated without correction. Most chemicals were purchased from Sigma Chemical Company (St. Louis, MO) or Aldrich Chemical Company (Milwaukee, WI).

Electrophysiology

Standard gigohm-seal recording techniques were used (Hamill, Marty, Neher, Sakmann, and Sigworth, 1981). Cells selected for recording were approximately spherical, and had input

TABLE 1A

Composition of Solutions

Name	Extracellular (bath) solutions						
	Na^+	K^+	Rb^+	Ca^{2+}	Mg^{2+}	Cl^-	HEPES
			mM				
Ringer's	160	4.5	0	2	1	170.5	5
160 Na	160	0	0	2	1	166	10
160 K	0	160	0	2	1	166	10
160 Rb	0	0	160	2	1	166	10
4.5 K + 160 Rb	0	4.5	160	2	1	170.5	5
160 K + 4.5 Rb	0	160	4.5	2	1	170.5	5

Mixtures of K^+ and Rb^+ are referred to as, *e.g.*, 40 K + 120 Rb, meaning 40 mM K^+ and 120 mM Rb^+ and were made by mixing appropriate amounts of 160 K and 160 Rb. Solutions with varying $[K^+]_o$ in which K^+ is the only permeant ion were made by combining appropriate amounts of 160 K and 160 Na. Solutions were titrated to pH 7.4 with the hydroxide of the predominant cation. HEPES is [4-(2-hydroxyethyl)-1-piperazineethane-sulfonic acid].

capacities of typically 10–15 pF. Standard conventions are used in all configurations, *i.e.*, outward current flowing from the intracellular to the extracellular side of the membrane is positive and is plotted as upward; applied clamp potentials which depolarize the intracellular side of the membrane are positive, and in the cell-attached patch configuration, potentials are stated relative to the cell's resting potential (RP) which is unknown, *e.g.*, RP + 80 mV means the membrane patch was depolarized by 80 mV above RP. Micropipettes were pulled in several stages using a Flaming Brown automatic pipette puller (Sutter Instruments, San Rafael, CA) from EG-6 glass (or infrequently from 0010 or KG-12 glass) obtained from Garner Glass Co. (Claremont, CA). Pipettes were coated with Sylgard 184 (Dow Corning Corp., Midland, MI), and heat polished to a tip resistance measured in Ringer's solution ranging typically between 0.9–1.8 MΩ. Electrical contact with the pipette solution was achieved by a thin sintered Ag-AgCl pellet (In Vivo Metric Systems, Healdsburg, CA) attached to a silver wire covered by a Teflon tube. Pipette and the initial bath solutions were filtered at 0.1–0.2 μm (Millipore Corp., Bedford, MA). A reference electrode made from a Ag-AgCl pellet was connected to the bath through an agar bridge saturated with Ringer's solution. The current signal from the patch

TABLE 1B

Composition of Solutions

Name	Intracellular (pipette) solutions							
	K^+	Cl^-	F^-	$CH_3SO_3^-$	Mg^{2+}	Ca^{2+}	EGTA	HEPES
*KCH_3SO_3	175	4	0	120	0	2	10	10
KCH_3SO_3+2 Mg	160	6	0	140	2	1	10	10
KCH_3SO_3/F	162	6	40	100	2	1	10	10
$NMGCH_3SO_3$	‡	4	0	160	2	0	5	5

*The KCH_3SO_3 solution also had 10 mM EDTA (ethylenediamine-tetraacetic acid).

‡Contains nominally 160 mM NMG^+ (*N*-methyl-D-glucamine).

K^+ solutions were titrated to pH 7.2–7.4 with KOH, $NMGCH_3SO_3$ solution was titrated to pH 7.0 with NMG^+. The dipotassium salt of EGTA, ethylene glycol bis-(β-aminoethyl ether) *N,N,N′,N′*-tetraacetic acid, was used in K^+ solutions. Monovalent cation concentrations are approximate and include estimates of the KOH or NMG^+ added to titrate the buffers present. Free $[Mg^{2+}]$ is ~1.9 mM in KCH_3SO_3+2 Mg and $NMGCH_3SO_3$, and <50 nM in the other pipette solutions (cf Silver and DeCoursey, 1990).

clamp (Axopatch-1A, Axon Instruments, Inc., Burlingame, CA) was recorded and analyzed using an Indec Laboratory Data Acquisition and Display System (Indec Corporation, Sunnyvale, CA). Series resistance compensation with the Axopatch-1A is prone to oscillation, and therefore was not used routinely. After whole-cell configuration was achieved by suction, the series resistance read from the dial was typically about double the pipette resistance in the bath (2–4 MΩ). The voltage error for a 1 nA current would be 2–4 mV, but most measurements of gating kinetics and voltage-dependence were done near V_{rev} where currents generally were smaller than this. Experiments were done at room temperature, with the bath temperature monitored continuously by a thinfilm platinum RTD (resistance temperature detector) element (Omega Engineering, Stamford, CT) immersed in the bath solution, and the temperature stored along with each record. Recorded bath temperature ranged 19–23°C, but was typically 21°C with a standard deviation of < 1°C for each data set in Table III. When extracted rate constants were plotted against temperature, the scatter in the data obscured any temperature effects, so the data were not corrected for temperature.

Data Analysis

Data were digitized and recorded in computer files for subsequent analysis. Analysis programs were written in BASIC-23 or in FORTRAN-77. The procedures for generating null-subtracted, averaged single-channel relaxations (Figs. 11, *A* and *B*) use programs written by Dr. Richard S. Lewis (Stanford University, CA) and are described fully elsewhere (Shapiro and DeCoursey, 1991*a*). Current relaxations were fitted by eye to exponential functions, while Boltzmann fits were by nonlinear least squares. Significance of differences were calculated by Student's two-tailed *t* test.

RESULTS

Inwardly rectifying K^+ (IR) channels have been observed in endothelial cells isolated from bovine pulmonary artery (Johns, Lategan, Lodge, Ryan, Van Breeman, and Adams, 1987; Cannell and Sage, 1989; Silver and DeCoursey, 1990), bovine aorta (Colden-Stanfield, Schilling, Ritchie, Eskin, Navarro, and Kunze, 1987; Takeda, Schini, and Stoeckel, 1987; Olesen, Davies, and Clapham, 1988), and human umbilical vein (Nilius and Reimann, 1990). Under the conditions of the present study of bovine pulmonary artery endothelial cells, the IR predominated whole-cell currents except in the positive potential range, and comprised the only obviously time-dependent conductance. Whole-cell currents during voltage ramps are plotted in Fig. 1. These ramp currents are equivalent to steady state current-voltage curves, except near V_{rev}, because of the rapidity of gating of the IR (Fig. 1, legend). In symmetrical K^+-containing solutions the IR gives rise to large inward currents with an approximately constant slope conductance, and a small hump of outward current positive to V_{rev} which vanishes 40–60 mV positive to V_{rev} (Adrian and Freygang, 1962). At more positive potentials there are outward currents unrelated to the IR which in the cell in Fig. 1 *A* are approximately linear and in the cell in Fig. 1 *B* increase progressively at large positive potentials. Some endothelial cells have a Cl^- conductance which under these ionic conditions would carry some outward current, and which is reduced but not eliminated when extracellular Cl^- is replaced by methanesulfonate$^-$ (Shapiro and DeCoursey, 1991*c*). In other cells there are increasing outward currents at quite positive potentials (as in Fig. 1 *B*) which are not reduced by replacement of Cl^- with methanesulfonate$^-$. Both of these conductances

are largely time-independent and are not affected when the IR is abolished by Ba^{2+} (Silver and DeCoursey, 1990), or when all external permeant cations are removed (160 Na trace in Fig. 1 *B*).

Rb^+ Block

Fig. 1 *A* illustrates superimposed whole-cell currents recorded during voltage ramps from −100 to +60 mV in a cell exposed to a wide range of $[Rb^+]_o$. The presence of even small amounts of Rb^+ in the external solution reduces inward currents through the IR. At each $[Rb^+]_o$ the fractional block at first increases at more negative potentials, indicating that Rb^+ block is voltage-dependent, but at large negative

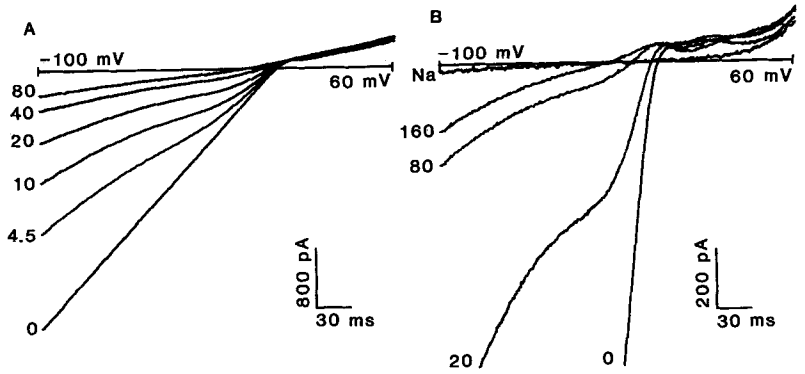

FIGURE 1. Whole-cell currents during voltage ramps in the indicated solutions, labeled according to the $[Rb^+]_o$ in mM with the remainder K^+, except for the trace in B labeled Na^+ which was permeant-free 160 Na. The voltage was ramped from −100 to 60 mV at 0.52 mV/ms. The pipette solution was KCH_3SO_3, bath temperature was 20.5°C (*A*) and 21.7°C (*B*). At both large negative and large positive potentials, these ramp currents are equivalent to steady state current-voltage curves, because gating of the IR is very fast (τ < 1 ms) more than 30 mV from $V_{1/2}$ in 160 K (Silver and DeCoursey, 1990). In the voltage range near V_{rev} where IR channel gating is slowest, some distortion will occur, especially in Rb^+-containing solutions in which gating is slower, because IR channels will open or close depending on the direction of the ramp. Even in 160 Rb, the maximum value for τ in most experiments is <30 ms, which is the time calibration bar in this figure.

potentials the blockade decreases again, with a weaker voltage dependence. Quite similar voltage-dependence of block was described by Standen and Stanfield (1980, their Fig. 2 *B*). That block does not continue to increase at large negative potentials suggests that Rb^+ can permeate IR channels, and that in this voltage range the blocking and unblocking rates have a similar voltage-dependence. The voltage-dependence of Rb^+ block can be estimated from the ratio of the current in the presence of Rb^+ to that in 160 K. Neglecting the gradual increase at large negative potentials (Standen and Stanfield, 1980), this ratio could be fitted by a Boltzmann function, with a midpoint shifting to more positive potentials as $[Rb^+]_o$ increased, and which limited to a minimum that decreased as $[Rb^+]_o$ increased. The slope factor

averaged 12.4 ± 2.7 mV (mean ± SD, n = 7) in 140 K + 20 Rb, and the potential at which half-block occurred was −2.7 ± 8.7 mV (n = 7).

Rb^+ Permeation

In Fig. 1 *B* ramp currents are shown at higher gain in another cell to illustrate the situation at high $[Rb^+]_o$. There are small inward currents in 80 K + 80 Rb, and smaller but qualitatively similar currents in 160 Rb. The small inward currents are much reduced when Rb^+ is replaced by Na^+. Evidently, Rb^+ can permeate IR channels. When only Rb^+ is present externally there is inward rectification (a superlinear *I–V* relationship) at large negative potentials which is eliminated in 160 Na. Inward rectification of pure Rb^+ current through the IR also occurs in other tissues (Hagiwara and Takahashi, 1974; Standen and Stanfield, 1980).

In high $[Rb^+]_o$ solutions in Fig. 1 *B*, there is a hump of outward current just positive to V_{rev}. In fact the slope conductance is greater for outward currents just positive to V_{rev} than for inward currents just negative to V_{rev}. This outward current hump is due to outward K^+ current (from the cell containing K^+) flowing through IR channels, because the hump disappears when Rb^+ is replaced by Na^+ (Fig. 1 *B*), and the behavior of the hump is consistent with the gating kinetics of the IR. Thus, when the potential is ramped more slowly the hump is reduced, because the channels have more time to close at a given potential. Ramping from positive to negative potentials eliminates the hump (not shown) because the IR channels are closed at positive potentials, and by the time they open the voltage is negative to V_{rev}.

Rb^+ Conductance with K^+-free Pipette Solution

The possibility that intracellular K^+ might interact with Rb^+ permeation led us to examine the Rb^+ conductance in endothelial cells using K^+-free pipette solutions. Whole-cell currents are illustrated in Fig. 2 in a cell dialyzed with $NMGCH_3SO_3$ (Table I*B*), during voltage ramps from +80 mV to −160 mV. When the bath solution was changed from Ringer's with 4.5 mM K^+ (not shown) to 160 K, the inward current increased ~20-fold, and outward current remained small. This behavior, together with the ubiquitous presence of large IR currents in endothelial cells, and the absence of other K^+-selective conductances at negative voltages with low intracellular free Ca^{2+}, supports the conclusion that these currents are due to IR channels. Changing the bath to 160 Rb greatly decreased the inward current (Fig. 2). Addition of 5 mM $BaCl_2$, an IR blocker, nearly abolished the inward current in 160 Rb, providing further support for the identity of the conductance as IR. The inward currents in 160 Rb were also greatly reduced by replacement with Na^+, TMA^+ (tetramethylammonium), or TEA^+ (tetraethylammonium). In conclusion, the Rb^+ conductance of the IR in endothelial cells is low regardless of the presence or absence of intracellular K^+.

Whole-cell currents in several Rb^+ and K^+ mixtures are also illustrated in Fig. 2. As in cells studied with K^+ in the pipette (Fig. 1), small additions of Rb^+ greatly reduced inward K^+ currents. One intriguing difference is that the enhancement of Rb^+ block by hyperpolarization was not observed in cells studied with K^+-free pipette solutions; instead the slope conductance increased monotonically with hyperpolarization at all $[Rb^+]_o$. The ratio of inward current in Rb^+-containing solutions to that in 160 K increased at more negative potentials. Block was only weakly voltage-dependent at

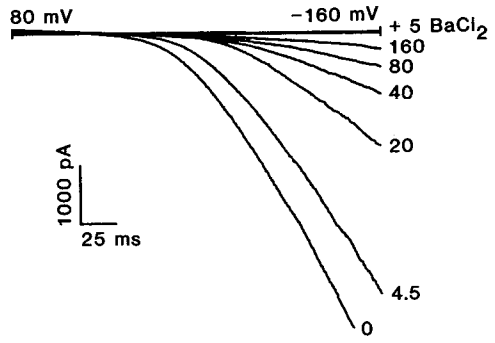

FIGURE 2. Whole-cell ramp currents in a cell with a permeant ion-free pipette solution, $NMGCH_3SO_3$ (Table I *B*). Note the lack of a region of decreased slope conductance, which was observed with K^+ in the cell (cf Fig. 1). The cell was held at 0 mV and the potential was ramped at a rate of −0.94 mV/ms from +80 mV to −160 mV every 8 s. $[Rb^+]_o$ is indicated near each record, and the horizontal line shows zero current. The current in 160 Rb solution with 5 mM $BaCl_2$ added, "+5 $BaCl_2$" is nearly superimposed on the voltage axis. The changes observed were rapidly reversible.

large negative potentials and similar to that with normal K^+ in the cell, but increased at more positive potentials. This is in contrast with the situation in normal $[K^+]_i$ where the opposite voltage-dependence was observed in the voltage range positive to −80 mV, namely relief of block by depolarization. This difference was not due to ramping "down" from positive to negative potentials, because ramping down with normal K^+ in the cell produced results indistinguishable from those when ramping up (except near V_{rev} where gating is slowest). Evidently intracellular K^+ relieves block at potentials near V_{rev}. Perhaps the relief of Rb^+ block in cells with normal $[K^+]_i$ reflects interactions of Rb^+ and internal K^+ within the channel.

Relative Conductance and Permeability

In Fig. 3 the ratio of current at −90 mV in the presence of various $[Rb^+]_o$ to the current in 160 K is plotted, both for cells with K^+ internally (◆) and for cells perfused

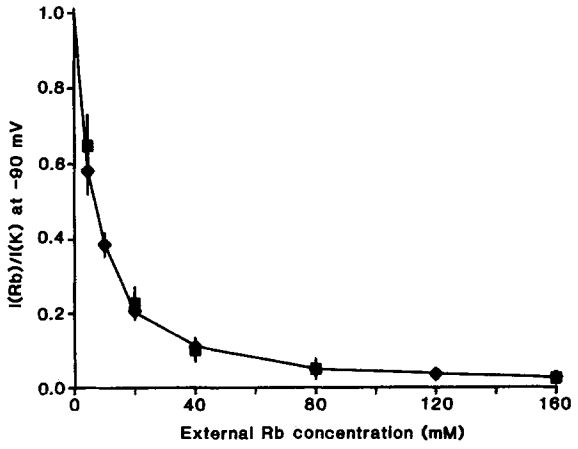

FIGURE 3. Reduction of IR current measured at −90 mV by increasing mole-fractions of Rb^+ in cells studied with high $[K^+]_i$ (KCH_3SO_3 solution, Table I *B*) (◆), and in cells studied with K^+-free pipette solution ($NMGCH_3SO_3$) (■). The IR current for a range of Rb^+ mole-fractions is expressed as a fraction of the current in the same cell in 160 K. Means ± 1 SD are plotted, for n = 4–6 (◆) and 2–8 (■). The measured currents were corrected for "leak" current also measured at −90 mV, defined as the current in permeant-free 160 Na solution or in 160 Rb + 5 $BaCl_2$. The block of IR currents by 5 mM Ba^{2+} was determined to be practically complete at −90 mV by comparison with current at that potential in the presence of 160 mM Na^+, TMA^+, or Cs^+.

with K^+-free pipette solution (■). Regardless of the internal solution, the reduction of inward current by Rb^+ is much greater than would result from simply replacing external K^+ with an inert impermeant ion. The current at −90 mV was reduced by 50% at < 10 mM Rb^+. Evidently, Rb^+ interferes with K^+ permeation. In three cells studied with high $[K^+]_i$, corrected for "leak" currents measured in permeant-free 160 Na, the conductance in 160 Rb relative to that in 160 K was 0.023 measured at V_{rev} − 20 mV and increased to 0.034 at V_{rev} − 80 mV. In cells perfused with K^+-free pipette solutions, the ratio of the slope conductance at −100 mV in 160 Rb to that in 160 K was 0.025 ± 0.009 (mean ± SD, n = 8), assuming that 5 mM $BaCl_2$ completely blocked the IR and can be used to estimate the leak. Thus, the relative conductance of Rb^+ at large negative potentials is the same whether or not K^+ is present internally. In contrast to the low conductance of Rb^+, when 160 K is replaced by 160 Rb (with K^+ present internally) V_{rev} shifted on average by −20.1 mV, indicating a permeability ratio P_{Rb}/P_K of 0.45 according to the Goldman-Hodgkin-Katz voltage equation.

Instantaneous Current-Voltage Relationships in Rb^+ and K^+

Macroscopic instantaneous *I–V* relationships could be determined up to a few tens of mV above V_{rev} in K^+-containing solutions. At 80 mM (Fig. 4 *A*) and 160 mM $[K^+]_o$ (data not shown), the *I–V* relation was approximately linear over the voltage range studied. The instantaneous *I–V* relation was somewhat easier to resolve in high $[Rb^+]_o$ because of the effects of Rb^+ on IR gating. In 80 K + 80 Rb (Fig. 4 *A*) inward currents were greatly reduced, with a smaller but substantial reduction of outward currents. The result is that the *I–V* relation rectifies strongly in the outward direction. The strong outward rectification at high $[Rb^+]_o$ is more obvious in Fig. 4 *B* in which the same data are plotted at higher gain, along with the *I–V* relation in the same experiment in 4.5 K + 160 Rb. In other experiments rectification in 160 Rb solutions was comparable to that in 4.5 K + 160 Rb, and in 160 K was similar to that in 80 K + 80 Na. In high $[Rb^+]_o$ the slope conductance for inward currents is 10–20 times smaller than that for outward currents. This ratio may slightly underestimate the extent of rectification, because the outward currents were corrected for time-independent leak current, whereas the inward currents were not corrected (see Fig. 4, legend), and the voltage range was limited. In intermediate $[Rb^+]_o$ solutions, *I–V* relations fell between these extremes.

K^+ and Rb^+ Permeation in Single IR Channels

IR currents in symmetrical K^+ in the cell-attached patch configuration. Inward rectifier currents were often observed in cell-attached patches after seals were formed in preparation for whole-cell experiments, using K^+-containing "internal" solutions (Table I *B*). Although several other types of channels were sometimes seen, IR channels have a characteristic behavior which makes their identification straightforward. One signature is that the open probability is high at negative potentials, whereas at positive potentials no outward current can be resolved. Fig. 5 illustrates the open-channel *i–V* relationship from an experiment in which conditions were maximized for detecting outward currents. The patch membrane was ramped rapidly from negative to positive potentials in order to increase the likelihood that the

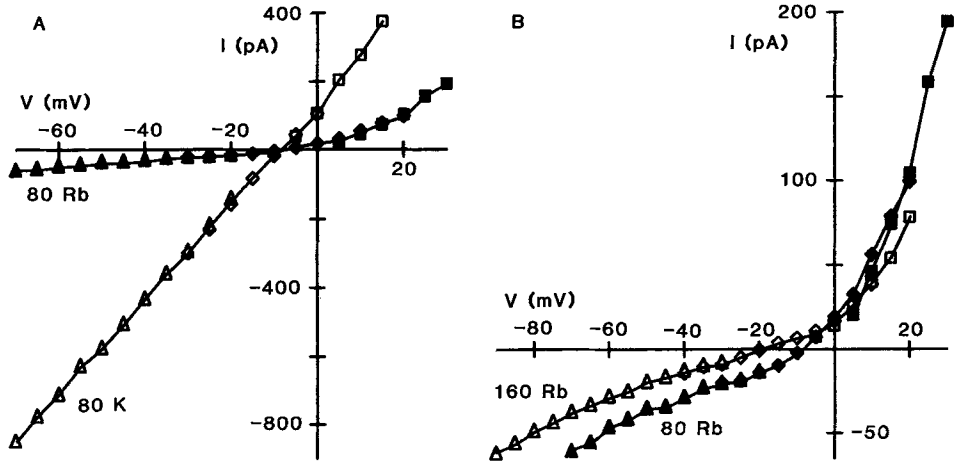

FIGURE 4. Instantaneous current-voltage relationships in 80 K + 80 Na (80 K, *open symbols*) and in 80 K + 80 Rb (80 Rb, *filled symbols*) (*A*), and at higher gain in the same cell in 4.5 K + 160 Rb (160 Rb, *open symbols*) and in 80 K + 80 Rb (80 Rb, *filled symbols*) (*B*) In all parts, triangles indicate peak currents during pulses to negative potentials at which the IR is fully activated, diamonds indicate directly measured instantaneous currents following negative prepulses which maximally activated the IR conductance, and squares indicate the amplitude of a single exponential fitted to the transient outward current following a prepulse. These last data are thus effectively corrected for any time-independent current unrelated to the IR, but for small depolarizations may underestimate the IR component if there are maintained outward currents. Pipette KCH_3SO_3, 22.4°C.

channel, open at negative potentials, would remain open during the ramp beyond V_{rev}. The single open-channel current was constructed by sorting and averaging sections of data in which the channel was open and sections in which the channel was closed, and subtracting the latter from the former. The slope conductance of the net open-channel current was 30 pS within ~60 mV of V_{rev} and increased to 42 pS at

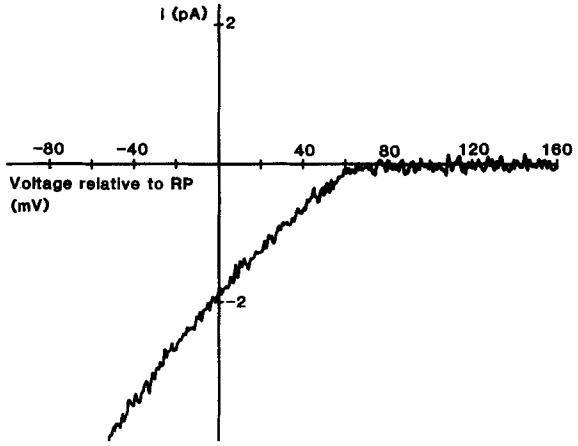

FIGURE 5. Averaged, leak-subtracted single open-channel current-voltage (*i–V*) relationship in a cell-attached patch, with KCH_3SO_3 in the pipette and Ringer's in the bath. Slope conductance at large negative potentials 42 pS. The patch membrane potential was ramped repeatedly from RP − 100 mV to RP + 160 mV at 5.08 mV/ms, sample interval 100 μs, ramp duration 50.8 ms, filter 2 kHz, 18.9°C. See text for details.

more negative potentials. In this experiment, and in all other cell-attached patch experiments, it was never possible to identify positively any instance of outward current through IR channels, either in voltage ramps or pulses. We attempted to enhance the signal-to-noise ratio by defining as "open" 50 ramp records in which the channel was open up to V_{rev}. The average obtained still showed no hint of outward current. In the cell-attached patch configuration, inward rectification of the IR channel appears to be absolute, within the resolution of our techniques.

IR currents in symmetrical K^+ in the outside-out patch configuration. In contrast to their behavior in cell-attached patches, IR channels in outside-out patches excised from endothelial cells can exhibit distinct outward current. In the experiment shown in Fig. 6 *A*, the voltage was ramped from negative to positive, and the average leak-subtracted open-channel *i–V* relation was found to be approximately linear with a conductance of 27 pS. The IR channel remained open up to +80 mV in only one record, so the data are noisy at positive potentials. During all other ramps the channel closed, as is evident from the averaged current from 60 sweeps, which is superimposed in this figure. The behavior of the averaged single-channel current is qualitatively similar to that of whole-cell macroscopic currents (*e.g.* Fig. 1), with a hump of outward current which vanishes 40–50 mV positive to V_{rev}. The outward current hump appears to be more pronounced in single channels in excised patches than at the whole-cell level.

Effects of $[Rb^+]_o$ on IR currents in the outside-out patch configuration. Single-channel IR currents in the presence of different $[Rb^+]_o$ were compared directly using outside-out patches. Three consecutive ramp records in 160 K are superimposed in Fig. 6 *B* (*darker lines*). About six IR channels were active, giving rise to the equivalent of scaled-down macroscopic IR currents. In 150 K + 10 Rb solution, the inward currents exhibited voltage-dependent block and were reduced by >50% at large negative potentials compared with 160 K (three consecutive traces are superimposed in Fig. 6 *B*), without any obvious change in the hump of outward current. The lack of change in outward current suggests that the same number of channels was open at negative potentials as in 160 K, that is, Rb^+ did not decrease the number or availability of functional IR channels. The reduction of inward current by 10 mM Rb^+ is comparable to its effect on whole-cell currents (Figs. 1 *A* and 3). Although single-channel current fluctuations are evident in Fig. 6 *B* in 160 K, in 150 K + 10 Rb unitary transitions were smaller and barely resolvable, the largest of which corresponded roughly with a conductance of 8–12 pS. Evidently, Rb^+ reduces the amplitude of single IR channel currents; if Rb^+ simply reduced the number of channels open at negative potentials without affecting the unitary conductance single-channel current levels would be the same size and as distinct as in 160 K. The lower conductance could be explained if each Rb^+ ion which permeates the channel transiently "blocks" the channel, *i.e.*, impedes the flow of K^+ through the channel, before passing through to the intracellular solution, with blocking kinetics too fast to permit resolution of discrete blocking events.

The number of functional IR channels in this patch declined with time. The unitary open-channel *i–V* relationships in Fig. 6 *A*, *C*, and *D* were recorded late in the experiment when only one or two channels remained active. When the solution bathing the outside-out patch was 80 K + 80 Rb or 160 Rb, unitary inward currents

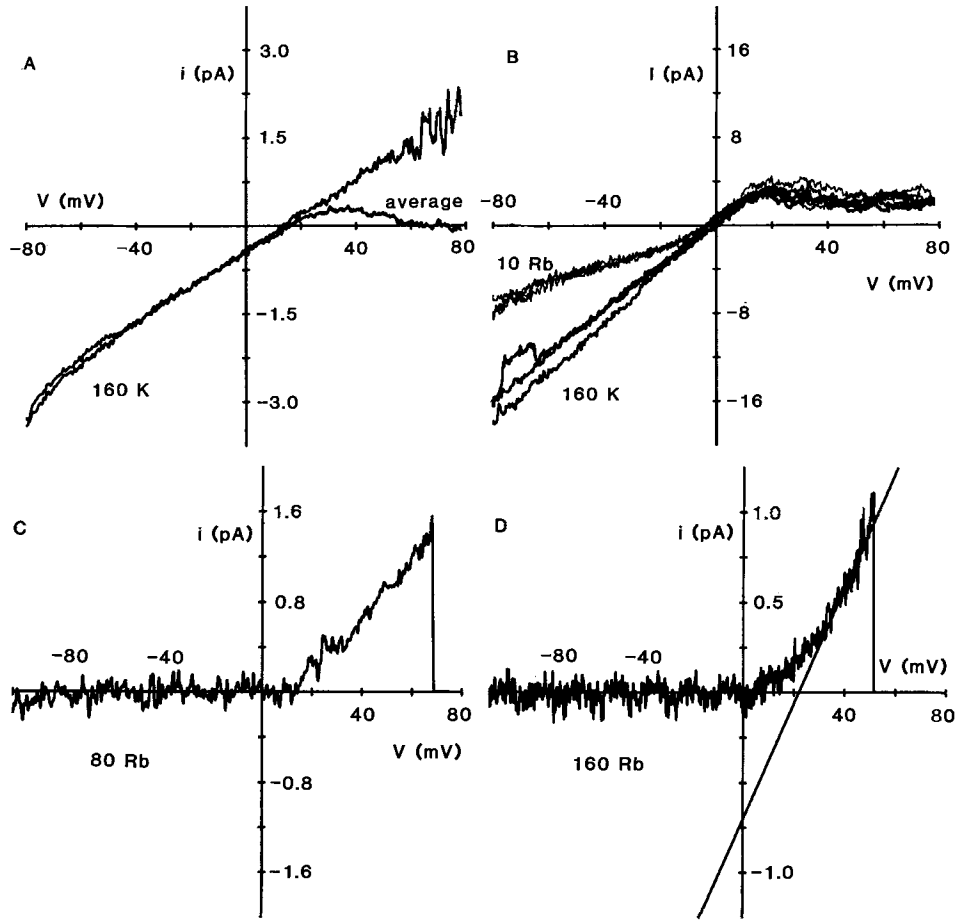

FIGURE 6. IR channel currents during voltage ramps in the same outside-out membrane patch, with nominally Mg^{2+}-free KCH_3SO_3/F in the pipette, and various solutions in the bath. After the patch was excised, the membrane resistance was high with <1 pA of leak current at ± 80 mV in permeant-free 160 Na.

(*A*) Unitary IR channel *i-V* relation with 160 K in the bath, after leak subtraction as described in Fig. 5. Superimposed is the leak-subtracted average current in 60 ramp records. The positive value of V_{rev}, +14 mV, in the presence of approximately symmetrical K^+ concentrations presumably reflects uncorrected liquid junction potentials and/or drift. Data collected 60 min after formation of the outside-out patch, when only one IR channel was active in the patch. Ramp rate 2.9 mV/ms, filter 2 kHz, holding potential +10 mV, 18.5°C.

(*B*) Currents during voltage ramps in 160 K (*dark lines*) and in 150 K + 10 Rb (*light lines*). Three records in each solution are superimposed, without leak correction. Note that, unlike the other parts of this figure, there are 4–6 IR channels open at the start of each ramp. Incomplete capacity compensation probably caused the current to reverse at more negative potentials (due to a small constant vertical offset) than in the other parts of this figure in which leak correction was applied. Recorded 20 min after patch excision. Ramp rate 1.8 mV/ms, filter 2 kHz, 21.4°C.

(*C*) Unitary IR channel current with 80 K + 80 Rb in the bath, leak-corrected as described in the text. No distinct inward currents were seen, but outward current events were observed

through the IR could not be detected, but outward currents could still be resolved. The net open-channel *i–V* relations are plotted in Figs. 6, *C* and *D*. Because IR channels close with depolarization the *i–V* relation could be determined only up to the most positive potential at which a channel remained open. Although inward unitary currents were not resolvable, it is clear that the open channel *i–V* relations exhibited strong outward rectification at high $[Rb^+]_o$. We attempted to estimate the unitary conductance for inward currents by sorting the ramp records according to whether the IR channel in the patch was open or closed above V_{rev}. If no opening was detectable the channels were considered "closed" in the negative range but "open" if a channel was open above V_{rev}. In 80 K + 80 Rb the estimated conductance was 1.1 pS, or 0.037 of the ~30 pS for the unitary IR conductance in 160 K. For comparison, the macroscopic current at −90 mV in 80 K + 80 Rb is 0.046 that in 160 K (Fig. 3). The procedure just described is obviously crude, and would underestimate the true conductance if there are records in which a channel was open at negative potentials but closed before the potential was enough beyond V_{rev} for outward current to be detectable. In 160 Rb (Fig. 6 *D*) the *i–V* relation rectifies strongly outwardly, consistent with the macroscopic instantaneous *I–V* relation in Fig. 4 *B*. Using the relative current estimate in 160 Rb in Fig. 3 of 0.027, the scaled unitary conductance would be only 0.8 pS in 160 Rb, a value below our resolution at the single channel level. In summary, in all solutions studied the rectification of single-channel currents qualitatively resembles the rectification of the macroscopic IR currents.

Effects of $[Rb^+]_o$ on the Voltage-dependence of IR Gating

Steady state voltage-dependence. The left inset in Fig. 7 illustrates the measurement of the steady state activation curve of the IR in 160 K (*cf* Silver and DeCoursey, 1990). Prepulses to a range of potentials were applied, which were long enough for the gating process to equilibrate, followed by a test pulse, in this case to −19 mV. The instantaneous current, obtained by extrapolating back to the start of the test pulse a single exponential curve fitted by eye to the test current, reflects the fraction of channels activated at the end of the prepulse. For large negative prepulses which fully activate the IR, the instantaneous test current is large, whereas after large positive prepulses which close IR channels, the test current is small initially and then rises to the same steady-state value. The instantaneous test current, plotted in Fig. 7 (■) after normalization to its fitted minimum and maximum values, reflects the

---

which tended to close at positive potentials. The voltage was ramped from −100 to +80 mV, but no channels stayed open above ~65 mV. The slope conductance by least-squares of the data from −100 to 0 mV is 1.1 pS, a value which should be regarded as very approximate; the slope conductance of the current positive to +37 mV is 26 pS. Recorded 53 min after patch excision, ramp speed 1.6 mV/ms, data sampled at 2 kHz and later Gaussian-filtered at 1 kHz, 18.3°C.

(*D*) Unitary IR channel current with 160 Rb in the bath. As in *C*, only outward currents were resolved and the data are leak-corrected. No channels remained open above ~50 mV. The slope conductance at positive potentials, indicated by the line, is 31 pS; that for inward currents is too small to calculate meaningfully. Recorded 43 min after patch excision, ramp speed 0.89 mV/ms, filter 1 kHz, holding potential 0 mV, 18.4°C.

voltage-dependence at steady-state of the gating mechanism of the IR. The original data were fitted to a Boltzmann function:

$$I_0(V) = (I_{0,max} - I_{0,min})/(1 + \exp(V - V_{1/2})/k) + I_{0,min} \quad (1)$$

where I_0 is the extrapolated instantaneous current at potential V, $I_{0,max}$ is the fitted maximum value of I_0, $I_{0,min}$ is the fitted minimum value of I_0, $V_{1/2}$ is the potential at

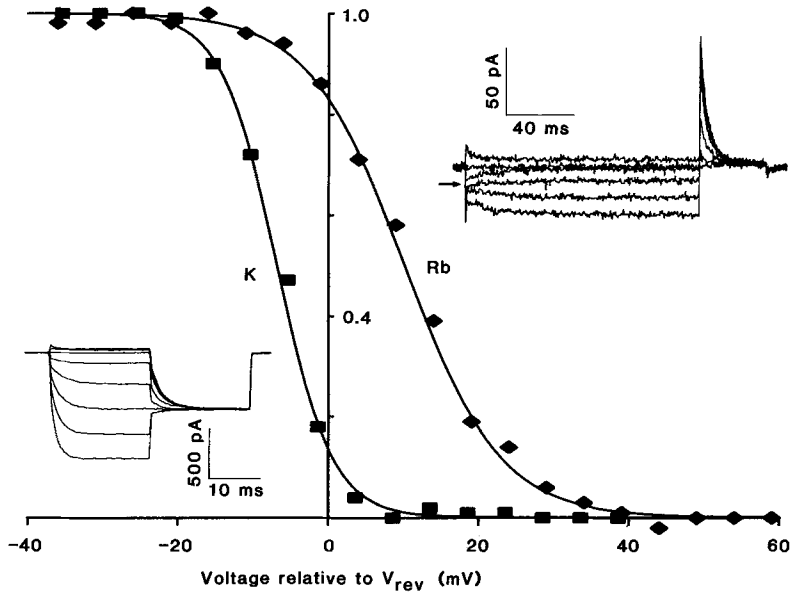

FIGURE 7. Steady state voltage-dependence of IR gating in a cell in 160 K (■) and in 160 Rb (◆). The amplitude of the activating (K^+) or deactivating (Rb^+) transients during the test pulses are plotted as a function of the prepulse potential. Data are normalized according to the fitted minimum and maximum for each data set, and the voltages on the abscissae are relative to the observed V_{rev} in each solution (−3.2 mV in 160 K and −27.1 mV in 160 Rb). Curves show fits to a Boltzmann function (Eq. 1), with midpoint $V_{1/2}$ and slope factor k in 160 Rb −16.5 mV (absolute potential) and 6.46 mV, respectively, and in 160 K, −9.7 and 3.72 mV. Pipette KCH_3SO_3. (*Left*) Measurement of activation curve in 160 K. Prepulses 20 ms long were applied from a holding potential of +1 mV, which was also the zero-current potential, followed by a test pulse to −19 mV. Illustrated prepulses are for −29 to +6 mV in 5 mV increments. Filter 2 kHz, sample interval 0.1 ms, 20.7°C. (*Right*) Measurement of activation curve in 160 Rb. Prepulses were 140 ms long, to allow full equilibration of gating, followed by a test pulse to +2 mV. Illustrated prepulses are to −43 to +7 mV in 10 mV increments. Arrow indicates zero current. Filter 2 kHz, sample interval 0.2 ms, 20.5°C.

which the IR conductance is half-activated, and k is a slope factor. Measured in 160 K (■), $V_{1/2}$ was 6.5 mV negative to V_{rev}. Note that the voltage axis is labelled relative to the reversal potential observed in each solution. The voltage dependence of gating is quite steep, with a slope factor, k of 3.7 mV. Mean values for these parameters in many cells are given in Table II. While the focus of the present study was on effects of Rb^+, we interspersed several measurements of the same cells in K^+-containing

solutions. As in our previous study (Silver and DeCoursey, 1990), $V_{1/2}$ was always negative to V_{rev} in K^+-containing, Rb^+-free solutions, and within the error of the measurement was displaced from V_{rev} by the same amount at all $[K^+]_o$ studied. Combining data at all $[K^+]_o$, $V_{1/2}$ was 6.9 mV negative to V_{rev} in the previous study (Table II, *top line*) and 6.0 mV in the present study (Table II, *third line*). The slope factor, k , was also similar in both data sets, 4.3 and 4.5 mV, respectively.

TABLE II

Steady State Voltage-dependence of IR Gating

$[K^+]_o$	$[Rb^+]_o$	$V_{1/2}$-V_{rev}	n	k	n
mM		*mV*		*mV*	
all*	0	−6.9 ± 0.7	39	4.3 ± 0.1	43
160*	0	−4.2 ± 1.4	5	4.4 ± 0.4	4
all	0	−6.0 ± 0.9	25	4.53 ± 0.19	25
160	0	−3.8 ± 2.0	3	4.17 ± 0.80	3
160	4.5	−6.4 ± 1.5	2	4.49 ± 0.68	2
150	10	−4.7 ± 1.4	5	4.30 ± 0.30	5
140	20	−5.8 ± 0.7	11	4.68 ± 0.40	11
120	40	‡n−3.8 ± 1.1	13	§n4.92 ± 0.16	13
80	80	‖1.5 ± 1.4	12	‖5.32 ± 0.10	12
40	120	‖6.8 ± 1.2	4	§‡5.68 ± 0.43	4
20	140	‖10.0 ± 2.1	5	‖5.87 ± 0.17	7
10	150	‖8.3 ± 2.6	6	‖6.19 ± 0.35	7
4.5	160	‖6.0 ± 0.6	19	‖6.48 ± 0.19	19
0	160	‖7.3 ± 2.2	6	‖6.16 ± 0.27	6

*Data from a previous study (Silver and DeCoursey, 1990) including only experiments with Mg^{2+}-free pipette solutions, as in the present study. Because both parameters were found to be identical for all $[K^+]_o$, values from $[K^+]_o$ ranging 4.5–160 mM are combined (*all*). Parameters defined in Eq. 1. Superscripted symbol pairs indicate significance levels in t tests vs control data in the top and third rows, respectively ($^‡ = p < 0.05$; $^‖ = p < 0.01$ for both controls; $^§ p < 0.01$; $^n p > 0.05$). Means ± SE are given for n = number of experiments.

Determination of the activation curve of the IR using the variable prepulse method in solutions containing high $[Rb^+]_o$ differed from that in solutions containing only K^+ in that the optimal test potential was positive to V_{rev}. The right-hand inset in Fig. 7 illustrates the measurement in 160 Rb in which the amplitude of the deactivating outward current was evaluated. Following negative prepulses the outward "tail current" is large, while after large depolarizing prepulses the amplitude of the test current is small. The extrapolated instantaneous current during the test pulse in 160 Rb is plotted in Fig. 7 (◆). The midpoint, $V_{1/2}$, was 10.6 mV positive to V_{rev}. When K^+ was replaced by Rb^+ in this experiment, V_{rev} changed by −24 mV while $V_{1/2}$ shifted only −7 mV. Table II summarizes the data at various $[Rb^+]_o$. As the Rb^+ mole-fraction increased and V_{rev} shifted to more negative potentials, $V_{1/2}$ changed more gradually, with the result that $V_{1/2}$ was well positive to V_{rev} in 160 Rb. As shown in Table II, this shift was significant at all $[Rb^+]_o > 40$ mM.

The voltage-dependence of IR gating was less steep in 160 Rb, with a slope factor of 6.5 mV in the cell in Fig. 7 compared with 3.7 mV in 160 K. Table II shows that, like $V_{1/2}$, k was significantly increased at $[Rb^+]_o > 40$ mM.

Effects of $[Rb^+]_o$ on macroscopic IR currents. Rb^+ greatly alters the appearance of IR current relaxations. The time-dependent activation of inward currents which is a hallmark of macroscopic IR currents in K^+-containing solutions is harder to resolve in high $[Rb^+]_o$. The cell in Fig. 8 *A* was held at −3 mV, well positive to V_{rev} at −26 mV. The current during the family of voltage steps exhibits small time-dependent relaxations. For the voltage steps negative to the holding potential, activating currents can be seen, which are outward at −8 and −18 mV and inward at more negative potentials because V_{rev} (indicated by an arrow) was −26 mV. Activation is

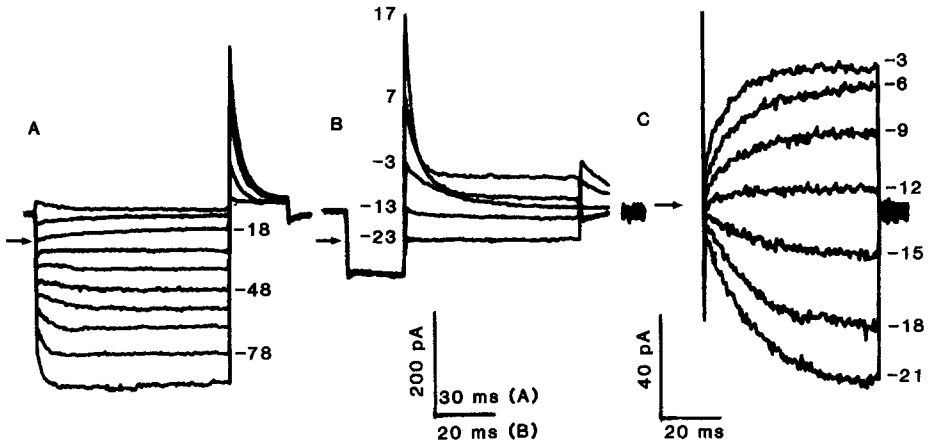

FIGURE 8. (*A*) Voltage dependent activation of whole-cell IR currents with 160 Rb in the bath and KCH_3SO_3 in the pipette. The cell membrane was held at −3 mV, stepped in 10 mV increments to +2 mV through −88 mV, followed by a 30-ms pulse to +6 mV. The extent of IR activation by these pulses can be assessed by examining the outward current transient during the pulse to +6 mV, as was illustrated in Fig. 7.

(*B*) Voltage-dependent deactivation of outward currents in the same cell as in *A*, also in 160 Rb. A prepulse 20 ms long to −43 mV was applied to activate the IR conductance, followed by depolarizing pulses to the indicated potentials, and then the potential was returned to −3 mV.

(*C*) Measurement of the reversal potential of the IR conductance, V_{rev}, in another cell in 80 K + 80 Rb solution. The cell was held at the zero-current potential which was −13 mV. A 20-ms prepulse was applied to +27 mV to deactivate the IR (current is off-scale), followed by test pulses 60 ms long to the indicated potentials. From the direction of IR current activation during these test pulses, V_{rev} was determined to be −13 mV. Arrows in all parts indicate zero current. All values have been corrected for liquid junction potentials (*see Materials and Methods*).

slower in 160 Rb than in K^+-containing solutions, and in both solutions becomes more rapid at more negative potentials. The decay of current during the most positive pulse (+2 mV) reflects deactivation of the IR conductance which was partially activated even in this cell held 23 mV positive to V_{rev}.

Fig. 8 *B* illustrates the kinetics of IR current deactivation in 160 Rb in the same cell as in Fig. 8 *A*. A hyperpolarizing prepulse activated the IR conductance, and then a range of test pulses were applied. Deactivation first becomes evident positive to V_{rev}, in contrast with K^+-containing solutions in which the IR conductance is already

largely deactivated at V_{rev}. The time constant of deactivation quantified by fitting the transient outward current with a single exponential becomes faster rapidly with further depolarization. Also observed in some experiments were smaller slowly-decaying outward currents, which might be due to the IR or to some other conductance.

V_{rev} in high $[Rb^+]_o$. A critical measurement in this study is that of V_{rev}, the reversal potential of the IR conductance. In high $[K^+]_o$ solutions in which V_{rev} is near 0 mV and the IR conductance is large compared with other conductances, the zero current potential corresponds closely with V_{rev}. However, in high $[Rb^+]_o$ where the IR conductance is greatly reduced and V_{rev} is more negative, leak or other extraneous conductances may introduce errors into the measurement. To determine V_{rev} as accurately as possible, we used the procedure illustrated in Fig. 8 *C*, in which a depolarizing prepulse which closed the IR channels (off-scale) was followed by a range of test pulses, and the current relaxation was observed. From the direction of the increase in IR current as channels open, V_{rev} can be determined. In the experiment in Fig. 8 *C* in 80 K + 80 Rb, the activating currents reversed at −13 mV. For this illustration 3 mV increments are shown, but for final determination of V_{rev} voltage increments of 1 mV were used. It is noteworthy that in Fig. 8 *C* distinct activation of outward current is evident, that is, there is significant steady state outward IR current in high $[Rb^+]_o$ solutions.

One of the classical behaviors of the IR, illustrated in Fig. 9 *A*, is that the voltage-dependence of activation shifts with V_{rev} when $[K^+]_o$ is varied, provided that $[K^+]_i$ is constant. At all $[K^+]_o$, $V_{1/2}$ (◆) was a few mV negative to V_{rev} (■). The same parameters are plotted in Fig. 9 *B* for various mole-fractions of Rb^+ and K^+. While V_{rev} was 20 mV more negative in 160 mM Rb^+ than in 160 mM K^+, $V_{1/2}$ barely changed. Thus, the two parameters became dissociated in the presence of Rb^+, and at $[Rb^+]_o > 80$ mM $V_{1/2}$ was positive to V_{rev}.

Effects of $[Rb^+]_o$ on the Gating Kinetics of the IR

Rb^+ slows IR gating. Macroscopic IR current relaxations, such as those in Fig. 8, were fitted with single exponentials over a range of Rb^+ mole fractions. Although small deviations from single exponential behavior were observed, no consistent pattern emerged. As was found previously for solutions containing various $[K^+]_o$, the τ-V relationship is bell-shaped, with a maximum near the midpoint of the activation curve. The relationship between $1/\tau$ and voltage is shown in Fig. 10 for a cell in 20 K + 140 Rb solution. Within the accuracy of the data, IR gating in all $[Rb^+]_o$ and $[K^+]_o$ mixtures could be expressed in the same form as in K^+-containing solutions, as a simple two-state system in which the opening rate, α, and the closing rate, β, are both exponentially dependent on voltage. The solid curve in Fig. 10 shows the fitted τ-V relationship, while the dotted lines show the components $\alpha(V)$ and $\beta(V)$, where

$$\alpha(V) = \bar{\alpha} \exp [(V_{1/2} - V)/k_\alpha] \quad (2)$$

and

$$\beta(V) = \bar{\beta} \exp [(V - V_{1/2})/k_\beta]. \quad (3)$$

The experimental values for α and β (shown as + and ×, respectively) were

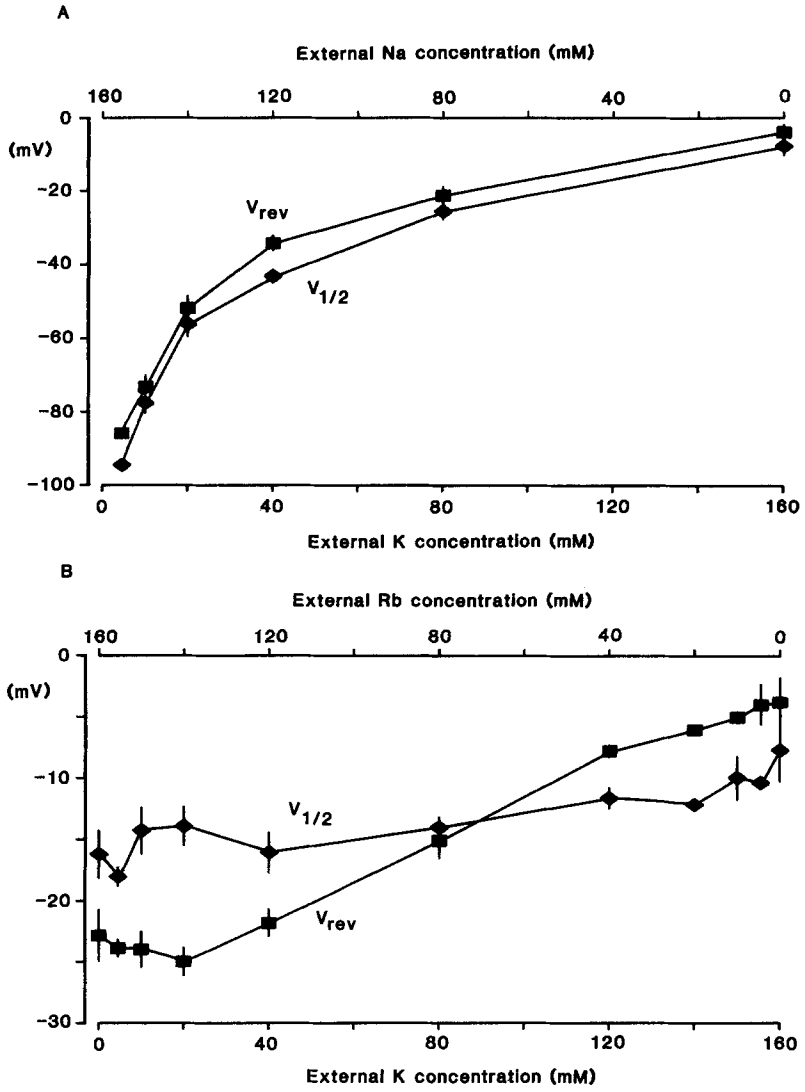

FIGURE 9. Comparison of the reversal potential, V_{rev} (■), and midpoint of activation of the IR, $V_{1/2}$ (◆), when $[K^+]_o$ was increased by substituting it for Na^+ (*A*) or Rb^+ (*B*). All values have been corrected for liquid junction potentials, and are plotted as mean ± 1 SE.

(*A*) The sum of $[K^+]_o$ and $[Na^+]_o$ for all solutions is 160 mM, except for Ringer's (Table I). Data from cells studied also in Rb^+ solutions were pooled with data from an earlier study (Silver and DeCoursey, 1990). Numbers of experiments, for increasing $[K^+]_o$, are: (V_{rev}: 23, 6, 5, 15, 8, 7; $V_{1/2}$: 23, 6, 5, 14, 8, 7).

(*B*) The sum of $[K^+]_o$ and $[Rb^+]_o$ is 160 mM, except for 4.5 K + 160 Rb and 160 K + 4.5 Rb (second data points from either end). Note that the ordinates encompass a smaller voltage range in *B*. Numbers of experiments, for decreasing $[Rb^+]_o$, starting with 160 mM $[Rb^+]_o$ are: (V_{rev}: 7, 21, 6, 6, 5, 15, 13, 10, 4, 2, 7; $V_{1/2}$: 6, 19, 7, 7, 4, 12, 13, 10, 4, 2, 7). The dependence of V_{rev} on $[K^+]_o$ and $[Rb^+]_o$ has an apparent minimum in the region of high $[Rb^+]_o$ and low $[K^+]_o$. Similar effects were noted by Hagiwara and Takahashi (1974). Based on P_{Rb} measured in 160 Rb, the Goldman-Hodgkin-Katz voltage equation predicts a monotonic relationship between Rb^+ mole-fraction and V_{rev}, with the calculated value for V_{rev} positive to the observed values in 80 mM and higher $[Rb^+]_o$. In six of nine cells in which V_{rev} was measured in 160 mM Rb^+ and at least one other solution in this range, V_{rev} was (anomalously) more negative at the lower $[Rb^+]_o$.

calculated from τ and P_{open}, the open probability derived from the fitted parameters of the activation curve, given that $\tau = 1/(\alpha + \beta)$ and $P_{open} = \alpha/(\alpha + \beta)$. We used $V_{1/2}$ as the reference potential for the rate constants, that is, $\bar{\alpha}$ and $\bar{\beta}$ are defined at $V_{1/2}$ in Eqs. 2 and 3. This procedure was adopted, as opposed to fixing the rate constants at their values at 0 mV for example, because when defined in this way their values were found previously to be independent of $[K^+]_o$ (Silver and DeCoursey, 1990). Table III gives the values for the rate constants and their slope factors, k_α and k_β, for the whole range of $[Rb^+]_o$ studied. The separation of the two rate constants, however, is not straightforward, because due to the nature of IR gating their extraction from the data is model-dependent (see Discussion). As defined here, Rb^+ reduced $\bar{\alpha}$ by a factor of 8, and $\bar{\beta}$ by a factor of 4. The voltage dependence of the opening rate, reflected in k_α, was significantly less steep in high $[Rb^+]_o$, whereas k_β was not altered.

Effect of Rb⁺ on deactivation kinetics in outside-out patches. The slowing of deactivation by Rb^+ was observable in isolated patches as well as in macroscopic

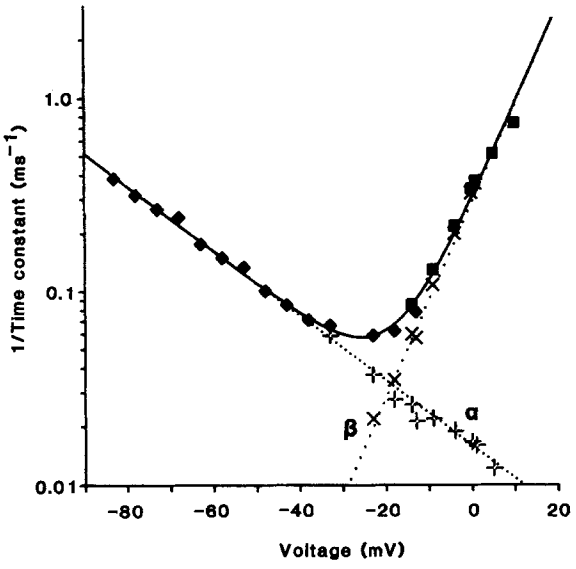

FIGURE 10. Extraction of IR rate constants from $1/\tau$ in 20 K + 140 Rb solution. Values for τ obtained by fitting macroscopic activation (◆) and deactivation (■) relaxations are plotted, along with values calculated for rate constants α (+) and β (×) using Eqs. 2 and 3, and activation curve parameters in this cell $V_{1/2}$ − 19.6 mV and k 6.6 mV. Fitted parameters were α 34.7 s^{-1}, k_α 26.1 mV, β 27.3 s^{-1}, k_β 8.74 mV, and $\alpha(V)$ and $\beta(V)$ are shown as dotted lines. V_{rev} was −28.3 mV in this cell. Pipette KCH_3SO_3, 20.9°C.

currents. It is difficult to resolve IR gating at the single-channel level even in K^+ solutions (Kurachi, 1985; Burton and Hutter, 1990), because gating occurs near V_{rev} where unitary currents are small. Here we consider only the strongly voltage- and $[K^+]_o$-dependent gating which corresponds with macroscopic IR activation/deactivation kinetics, and not the voltage-dependent inactivation of some IR channels at large negative potentials (Sakmann and Trube, 1984; Rae, 1986; Josephson and Brown, 1986; McKinney and Gallin, 1988). We could not resolve convincingly the activation kinetics of the IR at the single-channel level in high $[Rb^+]_o$. However, it was possible to resolve deactivation kinetics in isolated patches. The outside-out patch illustrated in Fig. 11 had many IR channels, with a steady state *I–V* relation measured in 160 K shown in Fig. 11 *C*. Deactivation was studied by applying depolarizing pulses from −20 mV, where the IR channels were maximally activated, to more positive potentials

at which the channels closed. Outward current transients composed of ensembles of many capacity-corrected records at +30 mV are shown in Fig. 11 *A* measured in 160 K, and in Fig. 11 *B* in 160 Rb. Both transients were well-fitted by a single-exponential decay, and the time constant, τ, was 3.1 ms in 160 K and 6.7 ms in Rb^+. Deactivation was slower in 160 Rb up to +60 mV at which point it was not clearly distinguishable from the capacity transient.

The voltage-dependence of IR gating kinetics in whole-cell experiments in 160 K and 160 Rb are summarized in Fig. 12. The curves show $1/\tau$ calculated from mean values for the rate constants, slope factors, and $V_{1/2}$ (indicated as tic marks). The

TABLE III

Rate Constants of IR Gating at 21°C

$[K^+]_o$	$[Rb^+]_o$	$\bar{\alpha}$	k_α	$\bar{\beta}$	k_β	n
mM		s^{-1}	*mV*	s^{-1}	*mV*	
all*	0	203. ± 14	17.7 ± 0.7	97. ± 6	9.0 ± 0.3	34
all	0	191. ± 13.5	19.0 ± 0.9	93. ± 15	7.5 ± 0.4	20, 17
160	0	211	16.9	61	5.5	2
160	4.5	263	22.3	138	7.8	1
150	10	195. ± 7	§‡24.4 ± 1.3	87. ± 14	7.4 ± 0.9	4
140	20	164. ± 12	‖28.1 ± 2.3	74. ± 13	7.5 ± 0.5	10, 5
120	40	‖104. ± 14	‖29.3 ± 1.2	§‡43.9 ± 6.5	§‡6.2 ± 0.4	13
80	80	‖51.1 ± 4.0	‖28.3 ± 1.5	‖31.4 ± 2.7	§ⁿ7.5 ± 0.4	14
40	120	‖22.8 ± 3.9	‡ⁿ22.7 ± 2.5	§ⁿ40.6 ± 11	9.2 ± 0.7	3, 5
20	140	‖31.8 ± 3.9	‖28.1 ± 0.8	‖24.2 ± 2.6	ⁿ‡9.3 ± 0.6	7
10	150	‖26.3 ± 3.4	‖26.1 ± 0.5	§‡24.1 ± 3.0	ⁿ‡9.3 ± 0.5	6
4.5	160	‖34.1 ± 2.4	‖25.5 ± 1.0	‖31.6 ± 2.6	ⁿ§9.4 ± 0.3	20
0	160	‖25.5 ± 3.7	‖26.9 ± 2.0	‖23.5 ± 3.0	ⁿ§10.0 ± 0.8	7

Parameters are defined as Eqs. 2 and 3. *Data from Silver and DeCoursey (1990) including only experiments with Mg^{2+}-free pipette solutions, as in the present study. Because all four kinetic parameters were found to be identical for all $[K^+]_o$, values for $[K^+]_o$ ranging 4.5–160 mM are combined. Symbol pairs indicate significance of differences vs control data in the first and second rows, respectively (‡ $p < 0.05$; § = $p < 0.01$; ‖ = $p < 0.01$ for both controls; ⁿ $p > 0.05$). Means ± SE are given for n = number of experiments; when two values for n are given the first value refers to $\bar{\alpha}$ and k_α and the second indicates $\bar{\beta}$ and k_β. Parameters related to activation ($\bar{\alpha}$, k_α) are more reliable than those for deactivation ($\bar{\beta}$, k_β) at low $[Rb^+]_o$, whereas the reverse is true at high $[Rb^+]_o$. Deactivation was particularly poorly-resolved at low $[Rb^+]_o$ and $1/\tau$ sometimes exhibited sublinear voltage-dependence at positive potentials, so k_β was poorly defined in these solutions. In most cases, the deactivation τ was determined directly from current transients (*e.g.*, Fig. 8 *B*), whereas in the earlier study, deactivation was generally determined from envolopes, which were considered more reliable in K^+-containing (*i.e.*, Rb^+-free) solutions.

voltage-axis is labeled in terms of absolute potential. Plotted in this way, deactivation (positive limb) is slowed in 160 Rb about twofold, in agreement with the single-channel deactivation ensembles in Fig. 11. Activation (negative limb) is slowed in 160 Rb by more than an order of magnitude, with the slowing effect increasing at more negative potentials. If the data are expressed relative to $V_{1/2}$, then the slowing of deactivation by Rb^+ is increased slightly, while that of activation is less; corresponding with the values given in Table III. Quantifying IR gating with reference to V_{rev}, because classically IR gating has been expressed as a function of $V–V_{rev}$, Rb^+ slows both α and β by about the same amount.

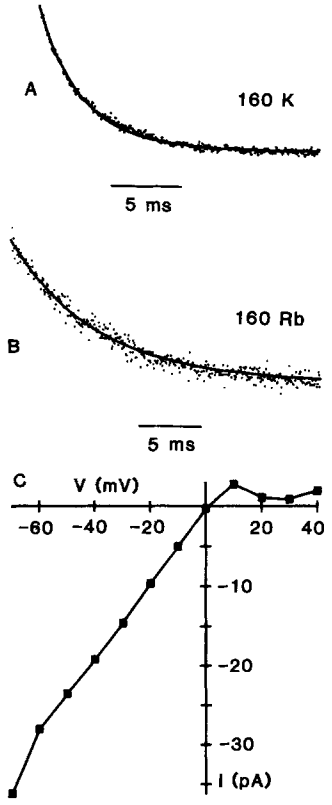

FIGURE 11. Ensemble IR channel tail currents in an excised outside-out patch in 160 K (*A*) and in 160 Rb (*B*) with KCH_3SO_3 + 2 Mg in the pipette. There were many IR channels in this patch. For both measurements, the patch was held at −20 mV (at which potential P_{open} was maximal) and repeated pulses to +30 mV were applied. To subtract capacity currents, the membrane was pulsed to −10 mV at which potential the g_K was still maximally activated, and the averaged data were then subtracted from the raw records at +30 mV after appropriate scaling. Superimposed on the data points are smooth curves showing the fit (by eye) to a single exponential, with τ = 6.7 ms in 160 Rb and 3.1 ms in 160 K. The amplitude of each transient was ~15 pA. In *A* and *B*, respectively, sample interval was 50 μs and 60 μs, 22.6°C and 22.0°C, 50 and 30 pulses averaged, filter 5 kHz in both. (*C*) Steady state *I–V* relationship of IR channels in the same outside-out patch with 160 K in the bath. Currents were measured at the end of 30 ms test pulses. Leak subtraction was based on scaled average currents during four repeated pulses, each ⅛ the amplitude of the test pulses, starting from a holding potential of +30 mV at which the channels appeared to be closed.

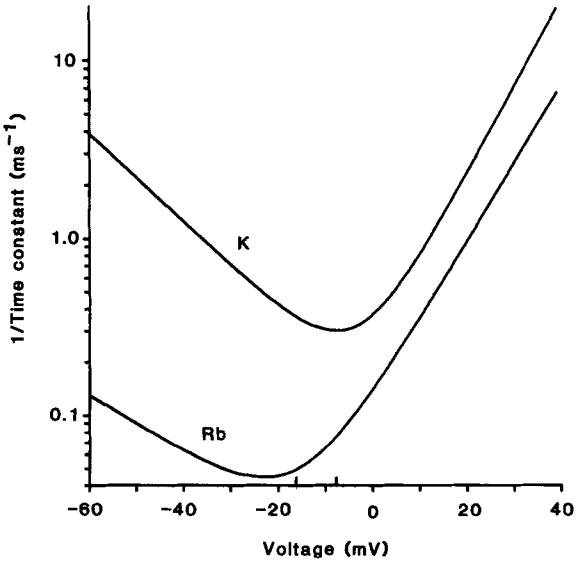

FIGURE 12. Voltage dependence of $1/\tau$ in 160 K (*upper curve*) and in 160 Rb (*lower curve*), calculated from mean parameter values for rate constants and slope factors. The rate constants given in Table III (top and bottom rows) are expressed relative to $V_{1/2}$, but this figure is plotted in terms of absolute potential; mean $V_{1/2}$ values in 160 K and 160 Rb are indicated on the *x*-axis by tic marks at −7.7 and −16.3 mV, respectively.

The mole-fraction dependence of the slowing of the rate constants by Rb^+ is plotted in Fig. 13. The effect of Rb^+ on the opening rate, α (◆), is greater than that on β (■), at least as these parameters were defined. Both parameters were reduced by small additions of Rb^+, approaching their limiting values in 160 Rb after ~50% of the K^+ was replaced by Rb^+.

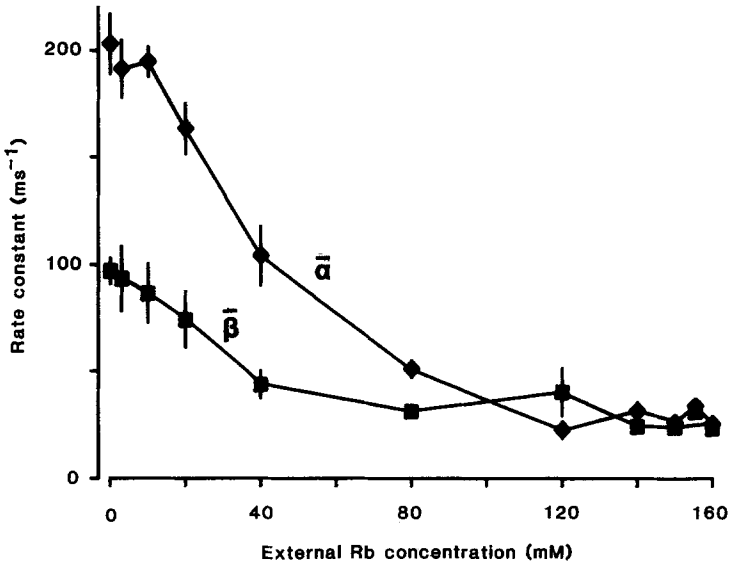

FIGURE 13. Effect of $[Rb^+]_o$ on the rate constants of IR gating, $\bar{\alpha}$ (◆) and $\bar{\beta}$ (■). Data from Table III are plotted ±1 SE. The data at 0 mM $[Rb^+]_o$ include all $[K^+]_o$ (4.5 to 160 mM) from Silver and DeCoursey (1990); for clarity new control data, also including all $[K^+]_o$, are plotted arbitrarily at 3 mM $[Rb^+]_o$.

DISCUSSION

Rb^+ Permeation Through IR Channels

Although Rb^+ has long been known to interfere with K^+ permeation through IR channels (Bolingbroke, Harris, and Sjodin, 1961; Adrian, 1964), it is not completely impermeant. Replacement of external K^+ with Rb^+ greatly reduces but does not abolish inward rectification, which can be further reduced by formaldehyde (Hutter and Williams, 1979), TEA^+ (Standen and Stanfield, 1980), or Ba^{2+} (this study). The relative permeability of Rb^+ in IR channels based on the Goldman-Hodgkin-Katz voltage equation is 0.3–0.4 in starfish egg cells, and the relative limiting slope conductance is 0.05 (Hagiwara and Takahashi, 1974). These values agree well with those obtained in the present study for macroscopic currents, with $P_{Rb}/P_K = 0.45$ and the relative Rb^+ conductance 0.034 at $V_{rev} - 80$ mV. Our results reconfirm that IR channels are more selective than most other voltage-dependent K^+ channels, such as various delayed rectifiers, whose P_{Rb}/P_K is >0.7 (references in Hille, 1992) and g_{Rb}/g_K under biionic conditions is ~0.5 (references in Shapiro and DeCoursey,

1991*a*). Consistent with the macroscopic instantaneous *I–V* relation, single channel rectification was strongly outward in outside-out patches with high $[Rb^+]_o$, that is, external Rb^+ greatly reduces inward currents but permits relatively large outward K^+ current through the IR. Lower Rb^+ mole fractions produce voltage-dependent reduction of the single-channel current consistent with effects on macroscopic current-voltage relationships.

In mixtures of Rb^+ and K^+ the inward IR current amplitude was reduced by small additions of Rb^+ more than expected if Rb^+ were simply an inert impermeant ion. Rb^+ in the external solution, while measurably permeant, evidently inhibits K^+ permeation through IR channels. In cells containing K^+, block by Rb^+ is enhanced by hyperpolarization at small negative potentials, reaching a limiting level of block which is relieved by extreme hyperpolarization. Similar voltage-dependent block by Rb^+ of IR channels in other preparations has been taken as evidence that Rb^+ blocks at a site within the pore (Hagiwara and Takahashi, 1974; Standen and Stanfield, 1980). The slope factor derived from the voltage dependence of the relative conductance in Rb^+-containing solutions, 10–16 mV, corresponds to an electrical distance, δ, in a one-site channel model (Woodhull, 1973) of 1.6–2.5, which suggests that the IR channel is multiply occupied by ions and that the block site is within the channel. When K^+-free pipette solutions were used, block at large negative potentials was similar in magnitude and voltage dependence to that with normal $[K^+]_i$. However, at less negative potentials block increased with depolarization when $[K^+]_i$ was low, but decreased with depolarization when $[K^+]_i$ was normal. Internal K^+ thus appears to relieve block by external Rb^+ at potentials approaching V_{rev}, even though the net current is inward. Similarly, Standen and Stanfield (1980) found that increasing $[K^+]_i$ reduced the affinity of Rb^+ for its block site in the IR of skeletal muscle. Voltage-dependent block by Rb^+ may be more accurately described as voltage-dependent interaction between external Rb^+ and internal K^+.

No time-dependence of block of macroscopic currents was detected, furthermore, the reduction of unitary current by Rb^+ occurred without detectable blocking events. Evidently Rb^+ block occurs at frequencies above the bandwidth of our recording. If the block site in the channel is occupied during permeation, then the minimum block rate can be estimated from the Rb^+ conductance in 160 Rb, using the scheme of Standen and Stanfield (1980):

$$Rb_o^+ + R \underset{k_{-1}}{\overset{k_1[Rb^+]_o}{\rightleftharpoons}} Rb^+R \underset{k_{-2}[Rb^+]_i}{\overset{k_2}{\rightleftharpoons}} Rb_i^+ + R,$$

where Rb_o^+ and Rb_i^+ represent a Rb^+ ion in the external or internal solution, R is the receptor site at which block occurs, and k_1, k_2, k_{-1}, and k_{-2} are rate constants. Because $[Rb^+]_i$ is assumed to be negligible in these experiments, $k_{-2}[Rb^+]_i$ is neglected. The unitary conductance at V_{rev}-90 mV, scaled according to Fig. 3, gives a net Rb^+ flux of 4.7×10^5 ions/s. If we take this as the rate Rb^+ exits the block site to the interior, k_2, then from the half-blocking concentration of $\sim$7 mM $[Rb^+]_o$ measured at −90 mV (Fig. 3), the forward block rate constant, k_1, is 6.7×10^7/M·s. This value represents the minimum rate of Rb^+ permeation/blocking events, which could be even higher if Rb^+ sometimes blocks a channel without permeating, if Rb^+ re-enters the channel from the inside, or if the block site is not continuously occupied in 160 Rb. That Rb^+

block is only weakly voltage-dependent at large negative potentials indicates that k_1 and k_2 either are both practically voltage-independent or have similar voltage-dependencies. For this analysis we assume the former possibility, and ascribe most of the voltage-dependence of block at potentials near $V_{1/2}$ to the rate that Rb^+ exits the block site to the external solution, k_{-1}. At large negative potentials k_{-1} is thus assumed to be negligible, so that $K_i \approx (k_{-1} + k_2)/k_1$ simplifies to $K_i \approx k_2/k_1$. The block rate constant for Rb^+ here, 6.7×10^7/M·s, is much higher than that reported by Matsuda, Matsuura, and Noma (1989), 1.75×10^6/M·s, for block of I_{K1} channels by Rb^+ at large negative potentials at 25°C. In that study, low concentrations of Rb^+ were used, 20–100 μM, in order to resolve single blocking events, which usually were all-or-none but sometimes produced subconductance levels. The higher block rate constant for endothelial cell IR channels and the higher $[Rb^+]_o$ used in the present study probably explain why we could not resolve discrete blocking events.

In contrast with the low Rb^+ conductance of the IR measured with high $[K^+]_i$ here and in other tissues (Hagiwara and Takahashi, 1974; Hutter and Williams, 1979; Standen and Stanfield, 1980), Mitra and Morad (1991) observed inward Rb^+ currents 51% as large as K^+ currents through the I_{K1} in cardiac myocytes studied with permeant ion-free pipette solutions. However, IR channels in endothelial cells exhibited the same low Rb^+ conductance of ~3% the K^+ conductance whether the cell was dialyzed with K^+ or impermeant NMG^+ pipette solutions. Evidently, the permeation properties of I_{K1} channels differ from those of IR channels of endothelial cells.

Effects of $[Rb^+]_o$ on the voltage-dependence and kinetics of IR gating. A major result of this study is that external Rb^+ shares with external K^+ the ability to establish the voltage-dependence of IR gating. Because of the well-known block of IR currents by Rb^+, we were at first surprised that it was possible to resolve IR gating at high $[Rb^+]_o$. As the Rb^+ mole-fraction increases and V_{rev} shifts to more negative potentials, $V_{1/2}$ changes more gradually, with the result that $V_{1/2}$ is well positive to V_{rev} in 160 Rb. The practical result is that in high $[Rb^+]_o$ most of the channels are open at V_{rev}, while in high $[K^+]_o$ most of the channels are closed at V_{rev}. This fact, combined with the slowing effect of Rb^+ on IR gating and the strong outward rectification when $[Rb^+]_o$ is large (Figs. 4 and 6), facilitated measuring the voltage-dependence of macroscopic IR gating in high $[Rb^+]_o$. The variable prepulse technique requires clear resolution of channel gating during the test pulse. In both Rb^+ and K^+ solutions, gating kinetics are slowest and therefore easiest to resolve near the midpoint of the activation curve; which in K^+-containing solutions is just negative to V_{rev} (*e.g.*, Hagiwara *et al.*, 1976; Leech and Stanfield, 1981; Tourneur *et al.*, 1987; Cohen *et al.*, 1989; Silver and DeCoursey, 1990), and in high $[Rb^+]_o$ is just positive to V_{rev}.

Because the voltage-dependence of IR gating depends strongly on $[K^+]_o$, we assume that the effects of Rb^+ are ascribable to binding of Rb^+ at the same site(s) at which K^+ affects gating. This site might be within the pore or at some external location remote from the permeation pathway. In cardiac myocytes external Cs^+ appears to share the ability of K^+ and Rb^+ in being able to activate I_{K1} channels (Mitra and Morad, 1991; Carmeliet, 1992). That external Rb^+ and K^+ strongly influence channel opening is consistent with the idea that the relevant gating sites are accessible from the external solution while the channel is closed. Spalding, Swift,

Senyk, and Horowicz (1982) reached similar conclusions from K^+ efflux studies in skeletal muscle. They found that in addition to its ability to inhibit K^+ efflux, presumably through IR channels, Rb^+ can also activate the IR like K^+ does by binding to externally accessible sites.

Both Rb^+ and Cs^+ slow I_{K1} activation measured at a fixed potential in cardiac myocytes (Tourneur *et al.*, 1987; Mitra and Morad, 1991). Rb^+ slows gating of the IR in endothelial cells as well, but evaluating whether opening or closing kinetics are altered is not straightforward. Because the IR has a voltage-dependence which depends strongly on external permeant ion concentrations, its conductance classically has been expressed as a function of $V-V_{rev}$ (*e.g.*, Hagiwara and Takahashi, 1974). The entire τ-V relationship (including both activation and deactivation) can be superimposed at any $[K^+]_o$ by shifting the data to superimpose $V_{1/2}$, and consequently we defined the rate constants with reference to that potential previously (Silver and DeCoursey, 1990) and in the present study (Table III). In contrast with the parallel shift of V_{rev} and $V_{1/2}$ when $[K^+]_o$ is changed, when $[Rb^+]_o$ is increased these parameters become dissociated. Thus the choice of $V_{1/2}$ (or V_{rev}) as a reference potential for extracting kinetic parameters becomes arbitrary. Referred to $V_{1/2}$ (Table III) $\bar{\alpha}$ was slowed (eightfold) more than $\bar{\beta}$ (fourfold) by Rb^+; referred to V_{rev} both α and β were slowed approximately equally; and expressed in terms of absolute potential (Fig. 12) the effect of Rb^+ was predominantly on $\alpha(V)$ (> 10-fold slowing) with only a twofold decrease in $\beta(V)$. If the voltage dependence of gating were set by a current-polarity-dependent mechanism, for example, then using V_{rev} as a reference point would be reasonable. Nevertheless, whether the rate constants are defined at V_{rev}, $V_{1/2}$, or at absolute potentials, both α and β are slowed by Rb^+.

Rb^+ also decreased the steepness of the voltage-dependence of steady state IR gating (k in Eq. 1 and Table II). The effective valence, $z\delta$, decreased from 5.8 (based on the weighted average value of k from previous and new data for all $[K^+]_o$) to 4.0 (combining data from the three highest $[Rb^+]_o$ which were indistinguishable from each other). Decomposition of the voltage-dependence of gating into that of channel opening (k_α) and channel closing (k_β) reveals that Rb^+ mainly affects the voltage-sensitivity of opening (42% increase in k_α, Table III) without affecting that of closing. The $z\delta$ derived from k_α was decreased from 1.4 in K^+ solutions to 1.0 at high $[Rb^+]_o$. The $z\delta$ derived from the steepness of the voltage-dependence of deactivation (k_β) in the present study was much higher than that of activation in both K^+ and high $[Rb^+]_o$ solutions, 3.0 and 2.7, respectively. Because the sum of $z\delta$ derived from k_α and k_β is somewhat less than that from the steady state activation curve (4.4 *vs* 5.8, respectively, for K^+ solutions and 3.7 *vs* 4.0 for high $[Rb^+]_o$), the voltage-dependence of at least one of the slope factors is likely underestimated, or the two-state model is inadequate.

Is a blocking particle model indicated? The possibility that the voltage-dependence of the IR might be due to an intracellular cationic blocking molecule has been considered by numerous investigators (Armstrong, 1969; Hagiwara and Takahashi, 1974; Hille and Schwarz, 1978; Vandenberg, 1987; Matsuda *et al.*, 1987). There are several examples in which a large molecule physically occludes the mouth of a K^+ channel, and the unblocking rate is increased by adding permeant ions to the opposite side of the channel. Internal quaternary ammonium ions block open K^+

channels and adding K^+ to the external side of the membrane promotes unblock (Armstrong, 1969, 1971; Armstrong and Hille, 1972). External charybdotoxin physically occludes Ca^{2+}-activated K^+ channels and is pushed off the blocking site by internal K^+ (MacKinnon and Miller, 1988). In a variety of K^+ channels inactivation is slowed while recovery from inactivation is accelerated by increasing $[K^+]_o$ (references cited in DeCoursey, 1990), which is consistent with K^+ influx destabilizing the NH_2-terminal region of the K^+ channel protein which acts as an inactivation particle (Zagotta, Hoshi, and Aldrich, 1990; Hoshi, Zagotta, and Aldrich, 1990) in a "ball-and-chain" model of inactivation (Armstrong and Bezanilla, 1977). Might IR gating be the result of an analogous mechanism in which gating is due to plugging the intracellular mouth of the pore by peptide residues comprising an intracellular portion of the IR channel protein? Occupancy of binding sites in the pore by permeant ions might destabilize the binding of a tethered blocking peptide. IR gating might then have the requisite dependence on $[K^+]_o$, with voltage dependence imparted by voltage-dependent occupancy of a site or sites within the pore.

The most severe difficulty with the intrinsic blocking particle model arises from the steepness of the voltage-dependence of IR gating, with an effective $z\delta$ of 3.1–5.9 (Leech and Stanfield, 1981; Tourneur *et al.*, 1987; Cohen *et al.*, 1989; Burton and Hutter, 1990; Silver and DeCoursey, 1990). Channel opening has a $z\delta$ of 1.4 in K^+ and 1.0 in high $[Rb^+]_o$ solutions. These latter values are similar to the voltage-dependence of unblocking in the examples cited above of K^+ displacing a blocking particle, with $z\delta \simeq 1.0$ (Armstrong, 1971; MacKinnon and Miller, 1988; Demo and Yellen, 1991). However, in these examples the onset of block/inactivation is practically voltage-independent; the analogous process, IR channel closing, in contrast is very steeply voltage-dependent. IR channel closing moves 2.7–3.0 equivalent charges across the membrane in K^+ and high $[Rb^+]_o$ solutions. From these examples of permeant ions ejecting blocking/gating moieties from superficial sites at the mouth of K^+ channels, we find no precedent to support the idea that an intrinsically voltage-independent gating process which does not involve a conformational change of the channel protein might gain sufficient voltage-dependence simply from the occupancy of permeant monovalent ions in the pore to account for IR gating.

Finding an effective $\delta > 1$ for ionic blockers classically has been taken as evidence that a channel is multiply occupied by ions during permeation (Hille and Schwarz, 1978). The largest $z\delta$ thus far reported for IR blockers is 1.5–1.6 for block by Cs^+ (Hagiwara *et al.*, 1976; Shioya, Matsuda, and Noma, 1993), 1.57 for Na^+ (Harvey and Ten Eick, 1989), and 1.6–2.5 for Rb^+ (present data); the largest value we are aware of for any other K^+ channel is 1.6 (see Hille and Schwarz, 1978). Steeper voltage-dependent block which is sensitive to $V-E_K$ can be produced by an impermeant blocking particle in a model long-pore, multi-ion channel, particularly if it is multivalent, but only at permeant ionic activities causing saturating occupancies (Hille and Schwarz, 1978). Nevertheless, even the divalent blocker Mg^{2+} within the IR channel itself has a $z\delta$ of only 1.14 (Matsuda, 1991). In summary, a simple blocking particle seems an unlikely mechanism for IR channel gating, although the gating mechanism may be modulated by occupancy of the channel. In the following paper (Pennefather and DeCoursey, 1994) we present an "electrochemical gating" model in which both K^+ and Rb^+ act as allosteric modulators of an intrinsically voltage-dependent isomerization between open and closed states of the IR channel.

Steep voltage and concentration dependence of IR activation is the result of required binding of several K^+ or Rb^+ to gating sites on the channel, in conjunction with cooperative gating of multiple bores of the channel.

Dependence of rectification on patch clamp configuration. The extent of outward current through single IR channels in patches was qualitatively different in cell-attached and excised outside-out patch configurations. No outward current could be detected in cell-attached patches under conditions designed to maximize it (Fig. 5). The absence of detectable outward current through IR channels in cell-attached patches has been reported in many cell types (*e.g.*, Sauve, Roy, and Payet, 1983; Sakmann and Trube, 1984; Rae, 1986; Vandenberg, 1987; Matsuda *et al.*, 1987; McKinney and Gallin, 1988). In contrast, outward current through IR channels was clearly evident in the outside-out patch configuration, both using a nominally Mg^{2+}-free pipette solution (Fig. 6) and one containing 1.9 mM Mg^{2+} (Fig. 11 *C*). Both steady-state and time-dependent outward currents were also detected in whole-cell experiments with high or low $[Mg^{2+}]_i$ (Silver and DeCoursey, 1990). In symmetrical K^+ the unitary *i–V* relation indeed is approximately linear, consistent with the observations of Vandenberg (1987) and Matsuda et al. (1987) in cardiac I_{K1} channels in inside-out patches. However, a gating process brings P_{open} to near 0 at large positive potentials, both with high and low $[Mg^{2+}]_i$. The behavior of single IR channels thus differs in cell-attached patches and in outside-out patches, and this difference is not entirely attributable to the presence or absence of internal Mg^{2+} in the outside-out patch. Deactivation of outward currents was slower in excised patches than at corresponding potentials in whole-cell experiments. Matsuda (1988) reported analogous progressive slowing of deactivation of I_{K1} channels in inside-out patches. This kinetic change in IR channel behavior may account for the enhanced outward current in excised patches. There may be an intracellular cofactor other than Mg^{2+}, which is lost after patch excision as suggested by Matsuda (1988), either attached to the channel protein or diffusible in the cytoplasm, that blocks outward currents or modulates the gating process.

An inward rectifier channel similar in most respects to that described here has been isolated and expressed recently in oocytes (Kubo *et al.*, 1993). It lacks the S4 segment believed to comprise the voltage sensor of depolarization-activated K^+ channels (Stühmer, Conti, Suzuki, Wang, Noda, Yahagi, Kubo, and Numa, 1989). Time-dependent current relaxations corresponding with the gating process described here were not detected, but may be resolved in future studies. It may be that macroscopic gating requires additional structures or post-translational modification of the channel. Site-directed mutagenesis may reveal whether the proposed gating-ion binding sites exist, and should provide additional evidence of the mechanism of IR gating.

The manuscript was greatly improved by thoughtful criticism by Drs. Bertil Hille and Peter Pennefather. We acknowledge the able technical assistance of Donald Anderson.

This work was supported by research grant HL37500 and Research Career Development Award KO4-1928 (Thomas E. DeCoursey), and NRSA pre-doctoral Training Grant HL07320 (Mark S. Shapiro) all from the National Institutes of Health, a Parker B. Francis Award (Michael R. Silver), and by Dr. Roger C. Bone.

Original version received 5 October 1992 and 24 October 1993.

REFERENCES

Adrian, R. H., and W. H. Freygang. 1962. Potassium conductance of frog muscle membrane under controlled voltage. *Journal of Physiology.* 163:104–114.

Adrian, R. H. 1964. The rubidium and potassium permeability of frog muscle membrane. *Journal of Physiology.* 175:134–159.

Almers, W. 1971. The potassium permeability of frog muscle membrane. PhD dissertation. University of Rochester, Rochester, NY.

Armstrong, C. M. 1969. Inactivation of the potassium conductance and related phenomena caused by quaternary ammonium ion injection in squid axons. *Journal of General Physiology.* 54:553–575.

Armstrong, C. M. 1971. Interaction of tetraethylammonium ion derivatives with the potassium channels of giant axons. *Journal of General Physiology.* 58:413–437.

Armstrong, C. M., and F. Bezanilla. 1977. Inactivation of the sodium channel. II. Gating current experiments. *Journal of General Physiology.* 70:567–590.

Armstrong, C. M., and B. Hille. 1972. The inner quaternary ammonium ion receptor in potassium channels of the node of Ranvier. *Journal of General Physiology.* 59:388–400.

Bolingbroke, V., E. J. Harris, and R. A. Sjodin. 1961. Rubidium and caesium entry, and cation interaction in frog skeletal muscle. *Journal of Physiology.* 157:289–305.

Burton, F. L., and O. F. Hutter. 1990. Sensitivity to flow of intrinsic gating in inwardly rectifying potassium channel from mammalian skeletal muscle. *Journal of Physiology.* 424:253–261.

Cannell, M. B., and S. O. Sage. 1989. Bradykinin-evoked changes in cytosolic calcium and membrane currents in cultured bovine pulmonary artery endothelial cells. *Journal of Physiology.* 419:555–568.

Carmeliet, E. 1992. Extracellular Cs^+ ions block but also activate K^+ current in cardiac myocytes. *Biophysical Journal.* 61:A251. (Abstr.)

Chen, D., and R. S. Eisenberg. 1992. Exchange diffusion, single filing, and gating in macroscopic channels of one conformation. *Journal of General Physiology.* 100:9*a*. (Abstr.)

Cohen, I. S., D. DiFrancesco, N. K. Mulrine, and P. Pennefather. 1989. Internal and external K^+ help gate the inward rectifier. *Biophysical Journal.* 55:197–202.

Colden-Stanfield, M., W. P. Schilling, A. K. Ritchie, S. G. Eskin, L. T. Navarro, and D. L. Kunze. 1987. Bradykinin-induced increases in cytosolic calcium and ionic currents in cultured bovine aortic endothelial cells. *Circulation Research.* 61:632–640.

DeCoursey, T. E. 1990. State-dependent inactivation of K^+ currents in rat type II alveolar epithelial cells. *Journal of General Physiology.* 95:617–646.

DeCoursey, T. E., J. Dempster, and O. F. Hutter. 1984. Inward rectifier current noise in frog skeletal muscle. *Journal of Physiology.* 349:299–327.

Demo, S. D., and G. Yellen. 1991. The inactivation gate of the *Shaker* K^+ channel behaves like an open-channel blocker. *Neuron.* 7:743–753.

Hagiwara, S., S. Miyazaki, S. Krasne, and S. Ciani. 1977. Anomalous permeabilities of the egg cell membrane of a starfish in K^+-Tl^+ mixtures. *Journal of General Physiology.* 70:269–281.

Hagiwara, S., S. Miyazaki, and N. P. Rosenthal. 1976. Potassium current and the effect of cesium on this current during anomalous rectification of the egg cell membrane of a starfish. *Journal of General Physiology.* 67:621–638.

Hagiwara, S., and K. Takahashi. 1974. The anomalous rectification and cation selectivity of the membrane of a starfish egg cell. *Journal of Membrane Biology.* 18:61–80.

Hagiwara, S., and M. Yoshii. 1979. Effects of internal potassium and sodium on the anomalous rectification of the starfish egg as examined by internal perfusion. *Journal of Physiology.* 292:251–265.

Hamill, O. P., A. Marty, E. Neher, B. Sakmann, and F. J. Sigworth. 1981. Improved patch-clamp techniques for high-resolution current recording from cells and cell-free membrane patches. *Pflügers Archiv.* 391:85–100.

Harvey, R. D., and R. E. Ten Eick. 1989. Voltage-dependent block of cardiac inward-rectifying potassium current by monovalent cations. *Journal of General Physiology.* 94:349–361.

Hestrin, S. 1981. The interaction of potassium with the activation of anomalous rectification in frog muscle membrane. *Journal of Physiology.* 317:497–508.

Hille, B. 1992. Ionic Channels of Excitable Membranes. Sinauer Associates, Sunderland, MA. 607 pp.

Hille, B., and W. Schwarz. 1978. Potassium channels as multi-ion single-file pores. *Journal of General Physiology.* 72:409–442.

Hodgkin, A. L., and P. Horowicz. 1959. The influence of potassium and chloride ions on the membrane potential of single muscle fibres. *Journal of Physiology.* 148:127–160.

Hoshi, T., W. N. Zagotta, and R. W. Aldrich. 1990. Biophysical and molecular mechanisms of *Shaker* potassium channel inactivation. *Science.* 250:533–538.

Hutter, O. F., and T. L. Williams. 1979. A dual effect of formaldehyde on the inwardly rectifying potassium conductance in skeletal muscle. *Journal of Physiology.* 286:591–606.

Johns, A., T. W. Lategan, N. J. Lodge, U. S. Ryan, C. Van Breeman, and D. J. Adams. 1987. Calcium entry through receptor-operated channels in bovine pulmonary artery endothelial cells. *Tissue and Cell.* 19:733–745.

Josephson, I. R., and A. M. Brown. 1986. Inwardly rectifying single-channel and whole cell K^+ currents in rat ventricular myocytes. *Journal of Membrane Biology.* 94:19–35.

Kubo, Y., T. J. Baldwin, Y. N. Jan, and L. Y. Jan. 1993. Primary structure and functional expression of a mouse inward rectifier potassium channel. *Nature.* 362:127–133.

Kurachi, Y. 1985. Voltage dependent activation of the inward rectifier potassium channel in the ventricular cell membrane of the guinea-pig heart. *Journal of Physiology.* 336:365–385.

Leech, C. A., and P. R. Stanfield. 1981. Inward rectification in frog skeletal muscle fibres and its dependence on membrane potential and external potassium. *Journal of Physiology.* 319:295–309.

MacKinnon, R., and C. Miller. 1988. Mechanism of charybdotoxin block of the high-conductance, Ca^{2+}-activated K^+ channel. *Journal of General Physiology.* 91:335–349.

Matsuda, H. 1988. Open-state substructure of inwardly rectifying potassium channels revealed by magnesium block in guinea-pig heart cells. *Journal of Physiology.* 397:237–258.

Matsuda, H. 1991. Effects of external and internal K^+ ions on magnesium block of inwardly rectifying K^+ channels in guinea-pig heart cells. *Journal of Physiology.* 435:83–99.

Matsuda, H., H. Matsuura, and A. Noma. 1989. Triple-barrel structure of inwardly rectifying K^+ channels revealed by Cs^+ and Rb^+ block in guinea-pig heart cells. *Journal of Physiology.* 413:139–157.

Matsuda, H., A. Saigusa, and H. Irisawa. 1987. Ohmic conductance through the inwardly rectifying K channel and blocking by internal Mg^{2+}. *Nature.* 325:156–159.

McKinney, L. C., and E. K. Gallin. 1988. Inwardly rectifying whole-cell and single-channel K currents in the murine macrophage cell line J774.1. *Journal of Membrane Biology.* 103:41–53.

Mitra, R. L., and M. Morad. 1991. Permeance of Cs^+ and Rb^+ through the inwardly rectifying K^+ channel in guinea pig ventricular myocytes. *Journal of Membrane Biology.* 122:33–42.

Nilius, B., and D. Riemann. 1990. Ion channels in human endothelial cells. *General Physiology and Biophysics.* 9:89–112.

Olesen, S. P., P. F. Davies, and D. E. Clapham. 1988. Muscarinic-activated K^+ current in bovine aortic endothelial cells. *Circulation Research.* 62:1059–1064.

Oliva, C., I. S. Cohen, and P. Pennefather. 1990. The mechanism of rectification of i_{K1} in canine Purkinje myocytes. *Journal of General Physiology.* 96:299–318.

Pennefather, P., and T. E. DeCoursey. 1994. A scheme to account for the effects of Rb^+ and K^+ on inward rectifier K-channels of bovine artery endothelial cells. *Journal of General Physiology.* 103:549–581.

Pennefather, P., C. Oliva, and N. Mulrine. 1992. Origin of the potassium and voltage dependence of the cardiac inwardly rectifying K-current (I_{K1}). *Biophysical Journal.* 61:448–462.

Rae, J. L. 1986. Potassium channels from chick lens epithelium. *Federation Proceedings.* 45:2718–2722.

Saigusa, A., and H. Matsuda. 1988. Outward currents through the inwardly rectifying potassium channel of guinea-pig ventricular cells. *Japanese Journal of Physiology.* 38:77–91.

Sakmann, B., and G. Trube. 1984. Conductance properties of single inwardly rectifying potassium channels in ventricular cells from guinea-pig heart. *Journal of Physiology.* 347:641–657.

Sauve, R., G. Roy, and D. Payet. 1983. Single channel K^+ currents from HeLa cells. *Journal of Membrane Biology.* 74:41–49.

Shapiro, M. S., and T. E. DeCoursey. 1991*a*. Selectivity and gating of the type L potassium channel in mouse lymphocytes. *Journal of General Physiology.* 97:1227–1250.

Shapiro, M. S., and T. E. DeCoursey. 1991*b*. Permeant ion effects on the gating of the type L potassium channel in mouse lymphocytes. *Journal of General Physiology.* 97:1251–1278.

Shapiro, M. S., and T. E. DeCoursey. 1991*c*. Chloride currents in bovine pulmonary artery endothelial cells. *In* Ion Channels of Vascular Smooth Muscle Cells and Endothelial Cells. N. Sperelakis and H. Kuriyama, editors. Elsevier Science Publishing Co., Inc., New York. 327–336.

Shioya, T., H. Matsuda, and A. Noma. 1993. Fast and slow blockades of the inward-rectifier K^+ channel by external divalent cations in guinea-pig cardiac myocytes. *Pflügers Archiv.* 422:427–435.

Silver, M. R., and T. E. DeCoursey. 1990. Intrinsic gating of inward rectifier in bovine pulmonary artery endothelial cells in the presence or absence of internal Mg^{2+}. *Journal of General Physiology.* 96:109–133.

Spalding, B. C., J. G. Swift, O. Senyk, and P. Horowicz. 1982. The dual effect of rubidium ions on potassium efflux in depolarized frog skeletal muscle. *Journal of Membrane Biology.* 69:145–157.

Standen, N. B., and P. R. Stanfield. 1980. Rubidium block and rubidium permeability of the inward rectifier of frog skeletal muscle. *Journal of Physiology.* 304:415–435.

Stanfield, P. R., F. M. Ashcroft, and T. D. Plant. 1981. Gating of a muscle K^+ channel and its dependence on the permeating ion species. *Nature.* 289:509–511.

Stühmer, W. F. Conti, H. Suzuki, X. Wang, M. Noda, N. Yahagi, H. Kubo, and S. Numa. 1989. Structural parts involved in activation and inactivation of the sodium channel. *Nature.* 339:597–603.

Takeda, K., V. Schini, and H. Stoeckel. 1987. Voltage-activated potassium, but not calcium currents in cultured bovine aortic endothelial cells. *Pflügers Archiv.* 410:385–393.

Tourneur, Y., R. Mitra, M. Morad, and O. Rougier. 1987. Activation properties of the inward-rectifying potassium channel of mammalian heart cells. *Journal of Membrane Biology.* 97:127–135.

Vandenberg, C. A. 1987. Inward rectification of a potassium channel in cardiac ventricular cells depends on internal magnesium ions. *Proceedings of the National Academy of Sciences, USA.* 84:2560–2564.

Woodhull, A. M. 1973. Ionic blockage of sodium channels in nerve. *Journal of General Physiology.* 61:687–708.

Zagotta, W. N., T. Hoshi, and R. W. Aldrich. 1990. Restoration of inactivation in mutants of *Shaker* potassium channels by a peptide derived from ShB. *Science.* 250:568–571.